3.2 TUBE SHEET ANALYSIS

3.2.1 DISCUSSION OF LOADING

The loading which was applied to the three dimensional model used in this study originated from the pressure history data previously described in Section 2.0. The pressure-time history was obtained for the primary coolant fluid, at the inlet and outlet sides of the primary face of the tubesheet. The break was applied in the loop analysis at the steam generator coolant outlet nozzle, and the flow from inlet to outlet side of the tubesheet was considered through an average tube. This is defined as that tube whose total length is the mathematical average of the length of all the tubes.

Figure 3.2-1 shows these time histories, and also that of the secondary side pressure, which is assumed to remain at an operating level of 964 psia throughout the transient. This figure provides the pressure differential considered to the worst case.

It can be seen that the primary outlet side experiences a step decrease in pressure of 1200 psi, while the primary inlet and secondary side pressures remains unchanged, within the first seven milliseconds.

Figure 3.2-2a shows the model, with the pressure loads at time equal to 0.0 seconds; Figure 3.2-2b shows the pressure loading at a time of 0.007 seconds, that time corresponding to the end of the step decrease. This latter representation, however, is not the loading which was statically analyzed. Due to the dynamic nature of the load, the pressure drop was amplified by a load factor of 2, this magnitude being defined in standard dynamics texts, e.g. Reference [15]. As a result, the three-dimensional model was statically loaded as shown in Figure 3.2-2c.

Due to the nature of the load, LOCA is defined as a Faulted Condition. Reference [10] prescribes that only stresses categorized as primary need be considered for Faulted Conditions. A uniform temperature of 600°F was designated as the reference temperature.

3.2.2 COMPUTATIONAL MODEL

The analysis of the Model D tubesheet under the LOCA loading was performed with the ANSYS computer code[16]. The model used was a three dimensional structure, consisting of the channel head, divider plate, tubesheet and stub barrel, (see Figures 3.2-2 through 3.2-4). Each of these component parts was represented by finite, flat, triangular shell elements. Interaction between these parts was obtained by coupling the displacements of common node points along their boundaries.

The corresponding three dimensional ANYSYS model is shown in Figures 3.2-5 through 3.2-13. As can be seen from these figures, the property of symmetry was employed and only half the structure was modeled.

In making the transition from the actual components to the three dimensional ANYSYS model, several assumptions were made. These were:

1. The penetration pattern of the model is a circular penetration area. In actuality, the Model D tubesheet penetration area is not circular, but contains several unperforated regions.

2. The U-tubes of the Model D steam generator are rolled into the entire thickness of the tubesheet, resulting in a stiffening effect on the tubesheet. In the calculation of the effective plate elastic constants, this fact was neglected.

3. It was assumed that the tubesheet would react to the LOCA loading primarily in one degree of freedom, that is, in the direction normal to its plane. This, however, was not a limitation which was imposed on the model, but rather a method of considering the application of a static load case representing the actual dynamic load history.

The finite element model incorporates the material properties of each of the component parts. The channel head is a carbon steel casting, designated SA-216 Grade WCC. Its material properties which are of interest in this study are the modulus of elasticity, E, and Poisson's Ratio ν.

Values of these properties at 600°F[10] are:

$$E = 25.7 \times 10^6 \text{ psi}$$
$$\nu = 0.3$$

The stub barrel is formed from low alloy steel plate designated SA-533 Grade A, Class 2. Its E and ν properties[10], are identical to those of the channel head.

The divider plate is a nickel-chrome-iron alloy, SB-168. Its material properties are 600°F[12] are:

$$E = 29.2 \times 10^6 \text{psi}$$
$$\nu = 0.3$$

The tubesheet is manufactured from an alloy steel forging designated SA-508 Class 2. The basic properties of the material are obtained from Reference [10]. However, the existence of the perforations necessitates modifying the elastic constants, so that the model employs an "equivalent" solid plate. The method used for this modification is described in Article A-8000 of Reference [10] and Reference [17]. Specifically the equivalent solid plate constants (denoted by an asterisk) imposed on the model were:

$$E^* = 0.43E = 11.05 \times 10^6 \text{ psi}$$
$$\nu^* = \nu = 0.3$$

3.2.3 STRESS LIMITS

The limitations on the tubesheet stresses induced by the LOCA loads, are those stress intensities categorized by Reference [10] as Primary in nature; i.e. Primary Membrane (P_M) and Primary Membrane plus Primary Bending ($P_M + P_B$).

The Primary membrane stress, in relation to a perforated plate, is the stress averaged across the ligament minimum width and through the thickness

of the plate. Also, the Primary membrane plus bending stresses, are those averaged across the ligament minimum width, but not through the thickness of the plate.

The stress limits imposed on the tubesheet under Faulted Condition limits are provided in the Appendix F Criteria[11]. For an elastic system with an elastic component analysis, the stress limits for nuclear components are:

P_m < the smaller of 2.4 S_m or 0.7 S_u
$P_m + P_B$ < the smaller of 3.6 S_m or 1.05 S_u

where

P_m = Primary Membrane Stress, psi
P_B = Primary Bending Stress, psi
S_m = Allowable Stress Intensity at temperature[10], psi
S_u = Ultimate stress from engineering stress-strain curve, at temperature, psi

The above limits assume a Shape Factor of 1.5 for the ligaments.

The values of these limits for the tubesheet material (SA-508 Cl. 2) at 600°F, for mechanical properties of,

S_m = 26.7 ksi
S_u = 80.0 ksi

are calculated as:

$P \leq 56.0$ ksi = 0.7 S_u
$P_m + P_B \leq 84.0$ ksi = 1.05 S_u

3.2.4 RESULTS

The results of the elastic analysis of the tubesheet of the Model D steam generator under the non-symmetric LOCA loads indicate that the stress intensities are within prescribed elastic limits.

The maximum Primary membrane plus Primary bending stress intensity occurs on a ligament on the secondary side of the inlet portion of the tubesheet, in the region defined by element 133 of Figure 3.2-17. The magnitude of this stress intensity is 25,200 psi and is well within the limit of 84,000 psi, for this stress category.

The maximum Primary membrane stress intensity can be found in the region of elements 107 and 108. These elements correspond to the region close to the center of the tubesheet--divider plate area, on the inlet side. The stress intensity was found to be 8,320 psi, much below the limit of 56,000 psi.

3.2.4.1 Effects of Individual Loads on Tubesheet

1. Pressure History

From the analysis of the model of the complete lower end of the steam generator, as shown in Figure 3.2-5, only the results affecting the tubesheet will be discussed. To further clarify the results, extra data is presented in the figures to display the general nature of the effect of LOCA loads and to substantiate expected trends. However, the basic objective of the tubesheet analysis is to show that the stresses developed under faulted conditions are below the limits specified in Section 3.2.3.

The perpendicular displacements of the tubesheet under the LOCA loading are shown in Figures 3.2-14 and 3.2-15. The first figure displays the shape of the tubesheet deflections, as they are plotted along a diameter and are relative to the tubesheet center. When comparing the inset in the figure, which shows the relative magnitudes of the pressure loads,

the tubesheet displacements is presented as expected. Figure 3.2-15 presents an isogram of the tubesheet deflections. This figure represents the tubesheet displacements in the middle surface of the tubesheet, as it appears in plan view.

The calculated equivalent bending stresses in the tubesheet are shown in Figure 3.2-16. This figure shows the radial stress in the tubesheet along a diameter perpendicular to the divider plate. As shown in the figure, the bending stress on the primary face of the tubesheet are generally compressive for that side on which the primary pressure dominates. On the outlet side of the primary face, the loading is dominated by the secondary side pressure, and the bending stresses on this side of the primary face are generally tensile. The stresses on the secondary face behave in the manner shown, which would be the predictable pattern when considering the pressure loads as shown in the inset diagram.

The irregular stress pattern at the center of the tubesheet is due to several factors. In this region, the model reflects the change in material properties, as displayed by the divider plate and the perforated tubesheet. In addition, there is an abrupt change of element caused by the attempt to accurately model this region. Both of these factors attenuate the results of the bending moment induced on the nodes in that area by the divider plate. Nevertheless, the general trend of the plots, especially that of the primary face, follows the expected pattern that would be caused by the pressure distribution used in this analysis.

Article A-8000 of Reference [10] provides stress analysis techniques for analyzing perforated plates. By modifying this method, due to the non-axisymmetric nature of the loads, the relationships of A-8142.1 can still be applied by considering the principle stresses σ_{max} and σ_{min} in place of σ_r and σ_θ, which are the equivalent solid plate radial and tangential stresses respectively. To obtain the ligament stresses on the tubesheet, the principle stresses were studied along six radial lines, as shown in Figure 3.2-17. Element stresses for the primary face, secondary face and midsurface regions of these lines were employed to calculate the

ligament stress intensities. Correlated by line number, Figures 3.2-18 through 20 are the ligament stress intensities due to the affect of the LOCA loading.

2. Tubesheet Response due to SSE and LOCA

The total transverse seismic force acting on the tubesheet is given by the product of the vertical acceleration and the mass of the tubesheet, plus the vertical reaction of the tube bundle.

The weight of the tubesheet, including enclosed primary water, is 65,300 pounds (169 lb-sec^2/in). The maximum relative tubesheet acceleration and tube bundle reaction were computed from the response spectrum analysis and are given in Table 3-2-1. The absolute acceleration of the tubesheet is obtained by adding the relative acceleration to the maximum vertical acceleration at the steam generator support points. The latter value is obtained from the response spectrum curve, Figure 2.3-1.

The maximum equivalent transverse bending stress σ that is expected to occur in the tubesheet during the SSE is computed by equation:[18]

$$\sigma = \frac{3(3+\nu)}{8h^2} pr^2$$

where

p = uniformily distributed transverse load
r = 68 in., radius of tubesheet
h = 21 in., thickness of tubesheet
ν = 0.2, equivalent Poisson's ratio

The above equation is based on the tubesheet being represented as a simply supported equivalent solid plate subjected to a uniform load. Since in reality, the tubesheet is partially constrained along its boundary, the stress computed by the simply supported formula is expected to be greater than the actual value. The maximum equivalent transverse bending stress, computed by the simply supported formula, is given in Table 3.2-1 as 126 psi, which is negligible.

Support movement of the steam generator due to blowdown forces, is of the same order at magnitude as that due to SSE. Consequently, stresses in the tubesheet induced by LOCA loads are also considered negligible.

TABLE 3.2-1

SSE TUBESHEET ACCELERATIONS

Component of Earthquake Motion	Horizontal Acceleration X	Horizontal Acceleration Y	Vertical Acceleration Z	Vertical Acceleration Σ
Relative vertical acceleration (in/sec^2)	10	8	142	160
Support vertical acceleration (in/sec^2)	0	0	206	206
Absolute vertical acceleration a(in/sec^2)	10	8	348	266
Tube bundle reaction R (lbs)	5020	4290	74700	84010

TUBESHEET SSE SEISMIC STRESS

Mass of tubesheet, m = 169 lb-sec^2/in

Total transverse load P = ma + R = 145,864 lbs

Total distributed load p = 10.04 lb/in^2

Maximum equivalent transverse bending stress = 126 psi

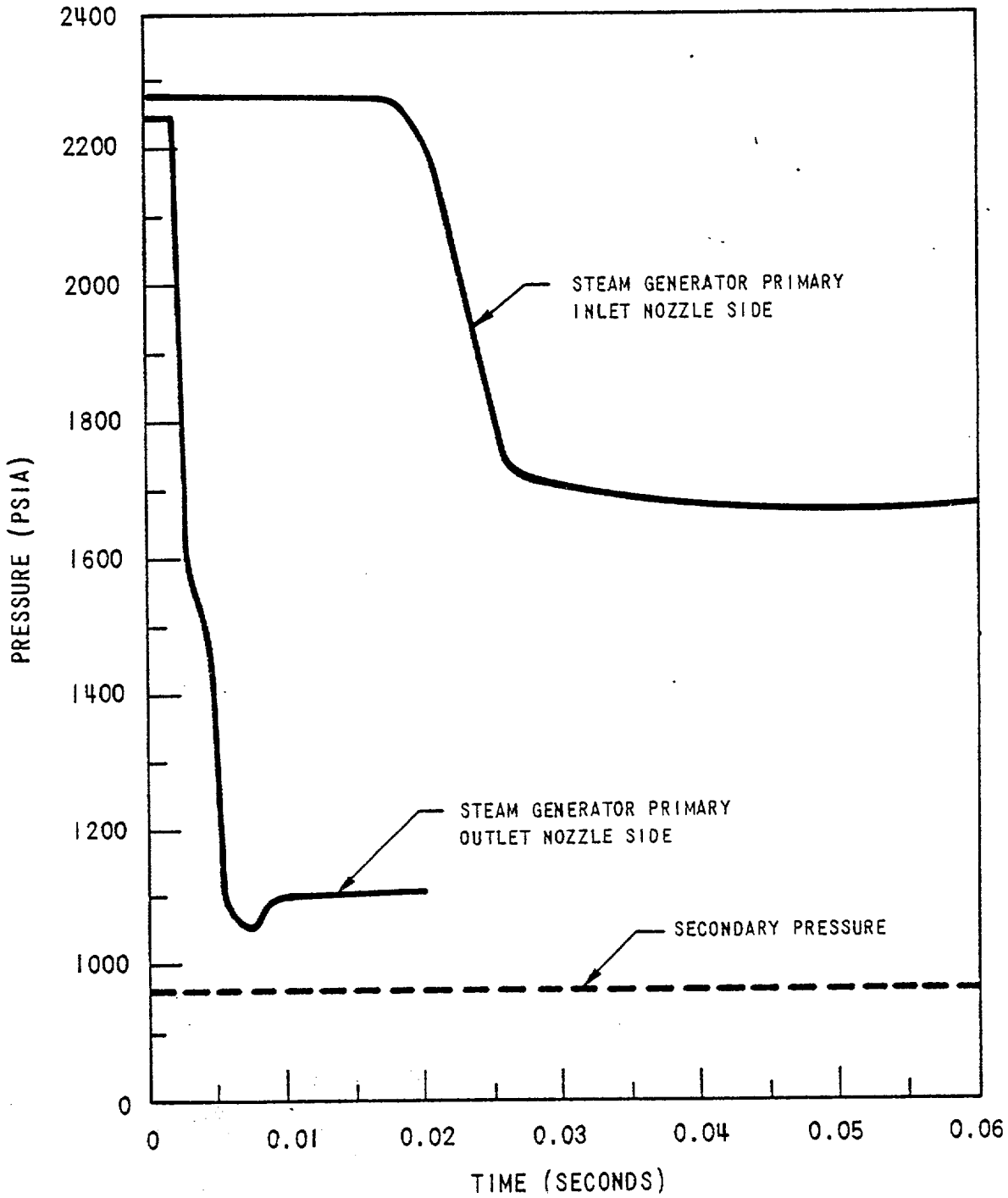

Figure 3.2-1 Pressure History at Tube Sheet During LOCA

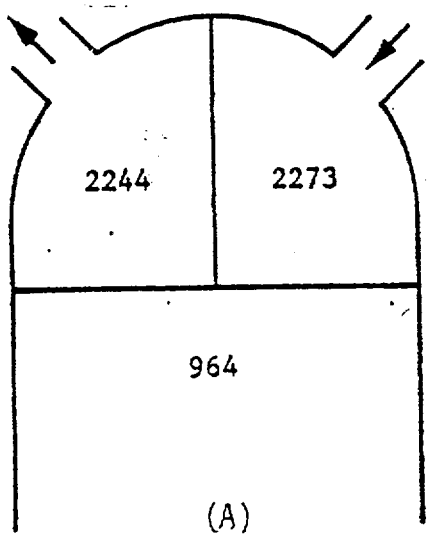

Pressure loads at t=0.0 sec.

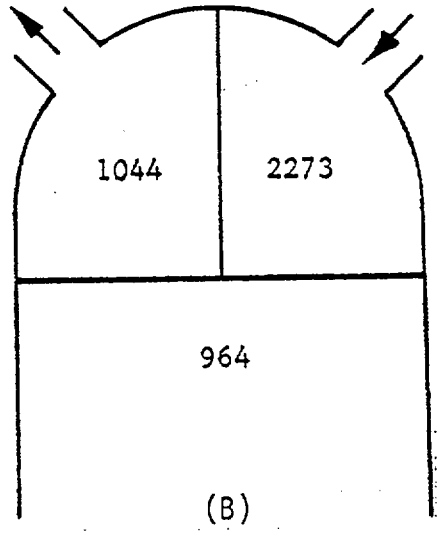

Pressure loads at t=0.007 sec.

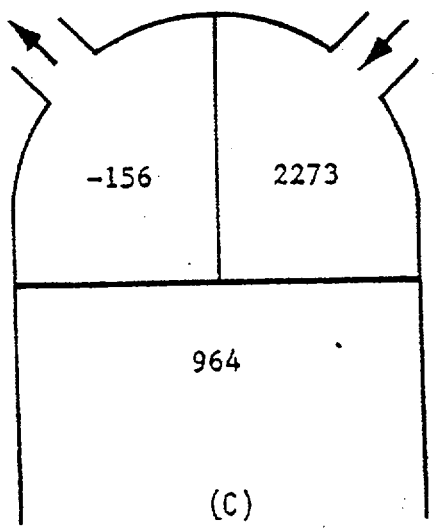

Pressure loads applied to static elastic model

Determination of static model pressure shown in (C)

1) 2244-1044=1200
2) Equivalent static pressure differential, using DLF=2.0, =2.0x1200=2400
3) Therefore, pressure in outlet plenum=+2244-2400=-156

Figure 3.2-2 Pressure Loads Due To LOCA

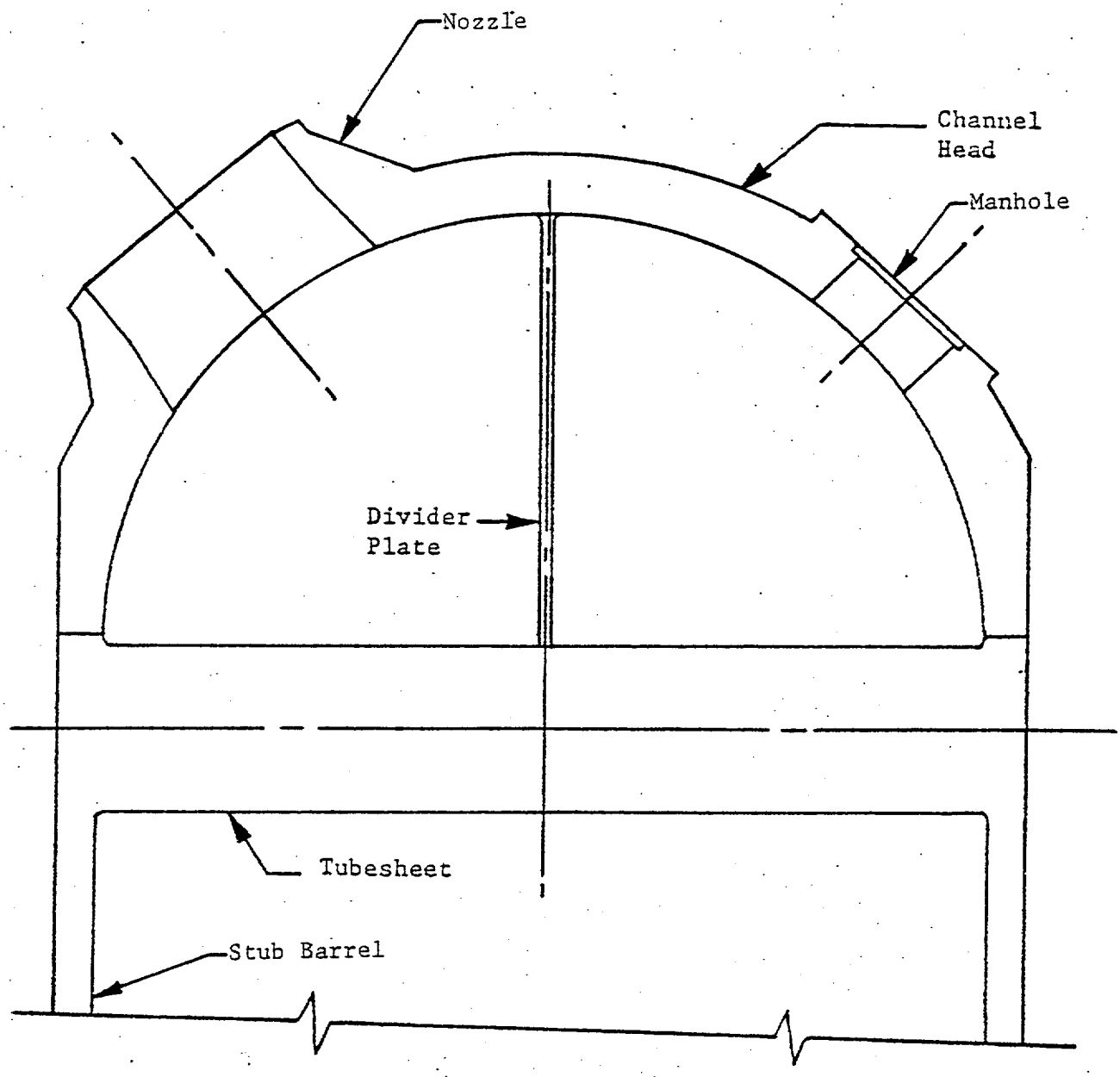

Figure 3.2-3 Channel Head, Tubesheet and Divider Plate Assembly

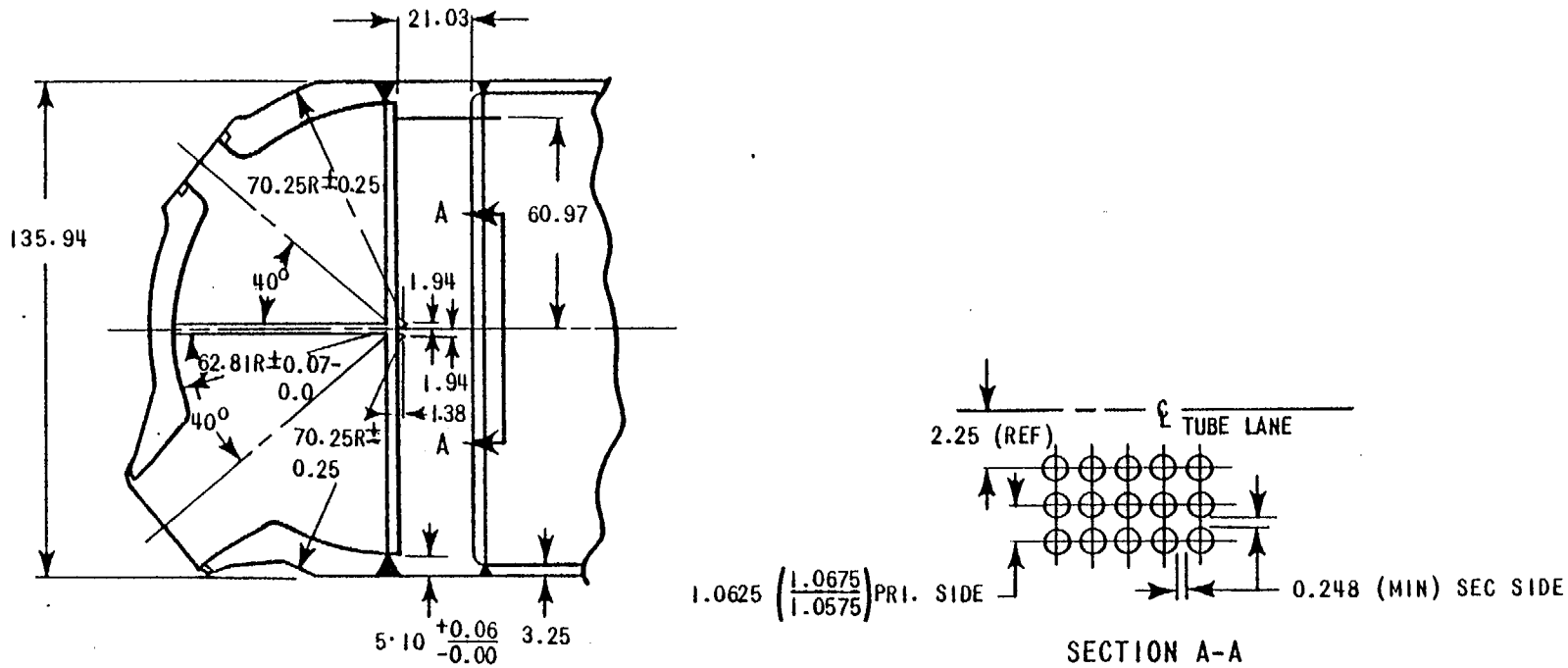

Figure 3.2-4. Tube Sheet-Channel Head-Stub Barrel Assembly Dimensions

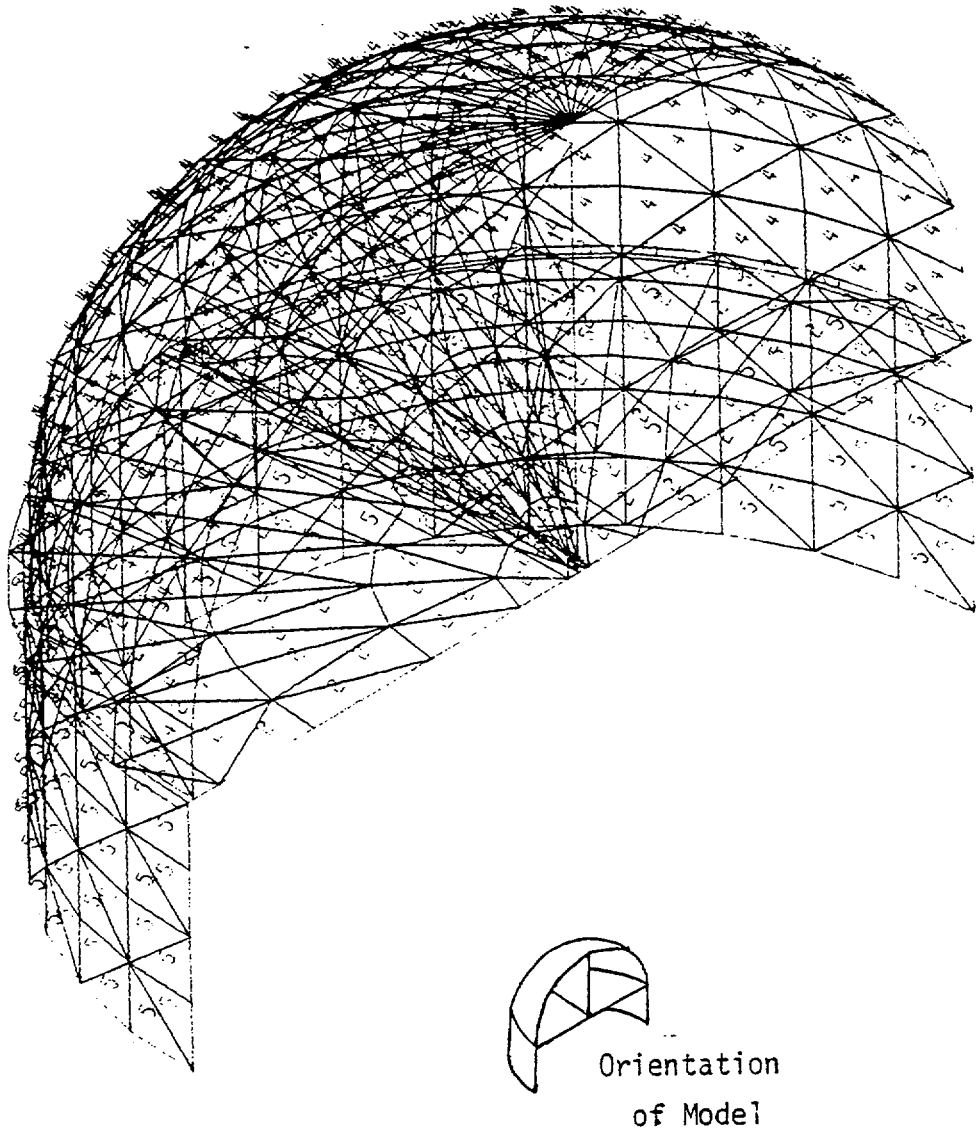

Figure 3.2-5 3-D ANSYS Model of (1) Divider Plate, (2&3) Tubesheet, (4) Channel Head and (5) Stub Barrel.

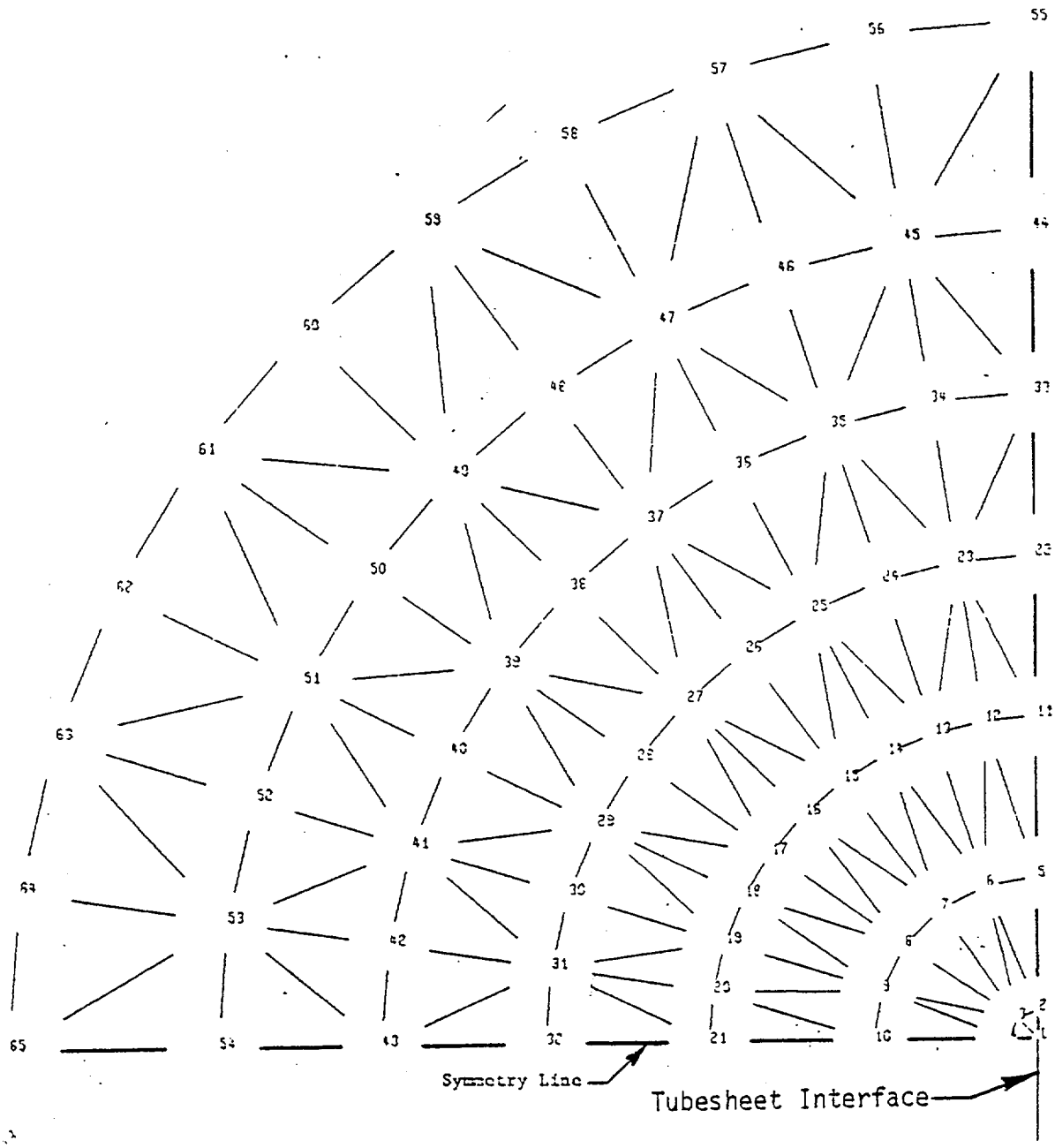

Figure 3.2-6 Node Points, Divider Plate Portion of 3-D ANSYS Model

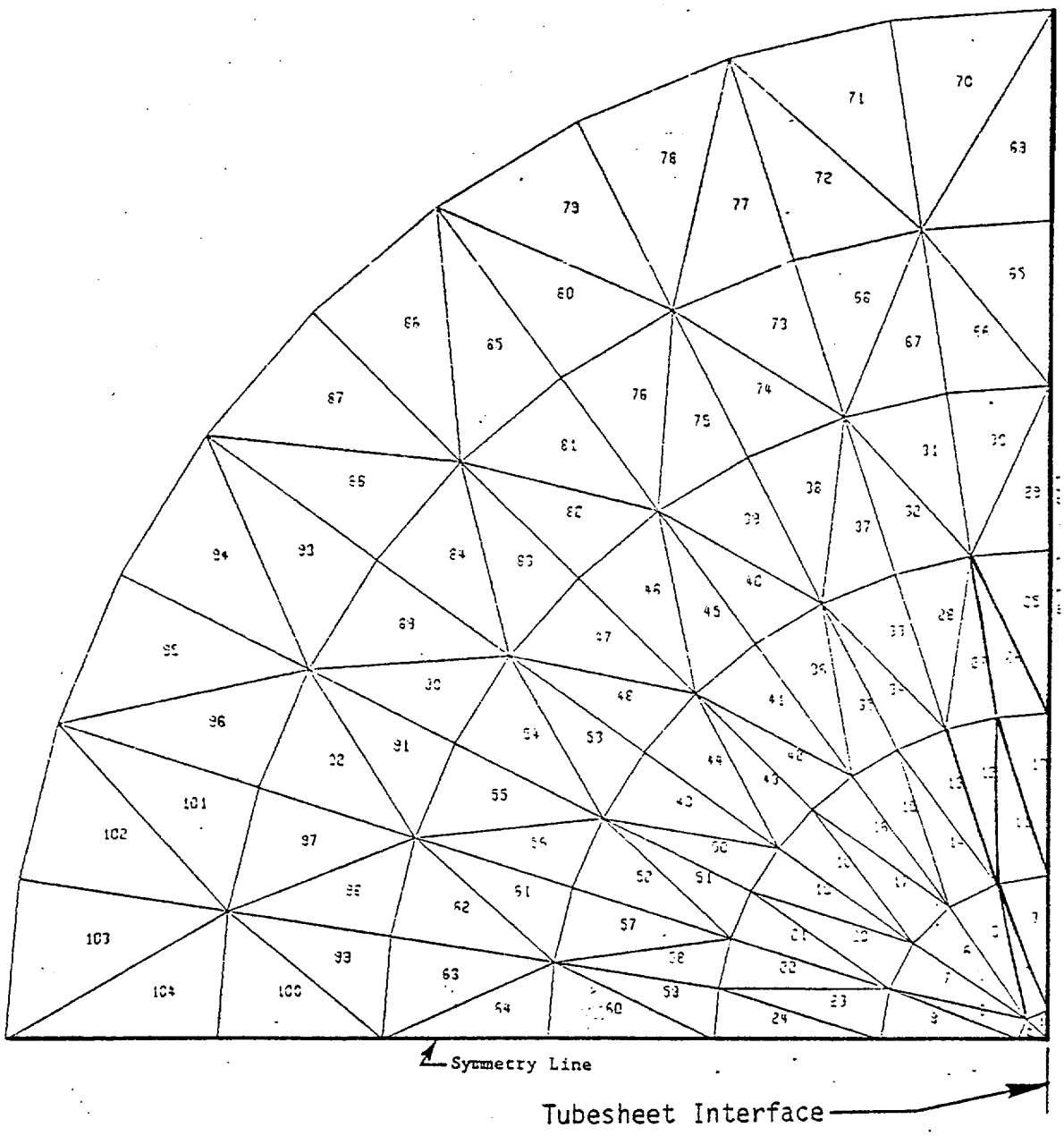

Figure 3.2-7 Elements, Divider Plate Portion of 3-D ANSYS Model

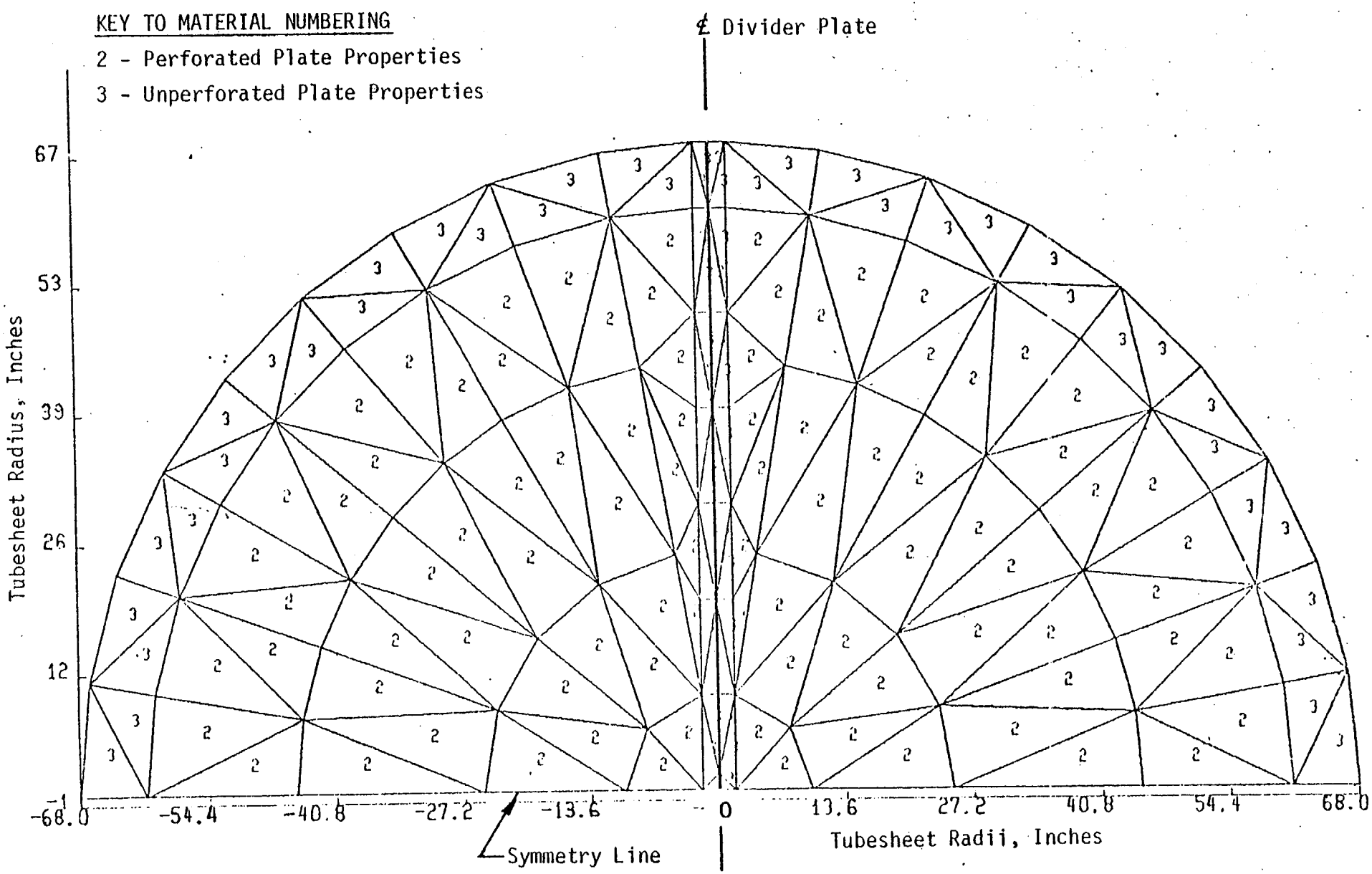

Figure 3.2-8 Tubesheet Properties, 3-D ANSYS Model

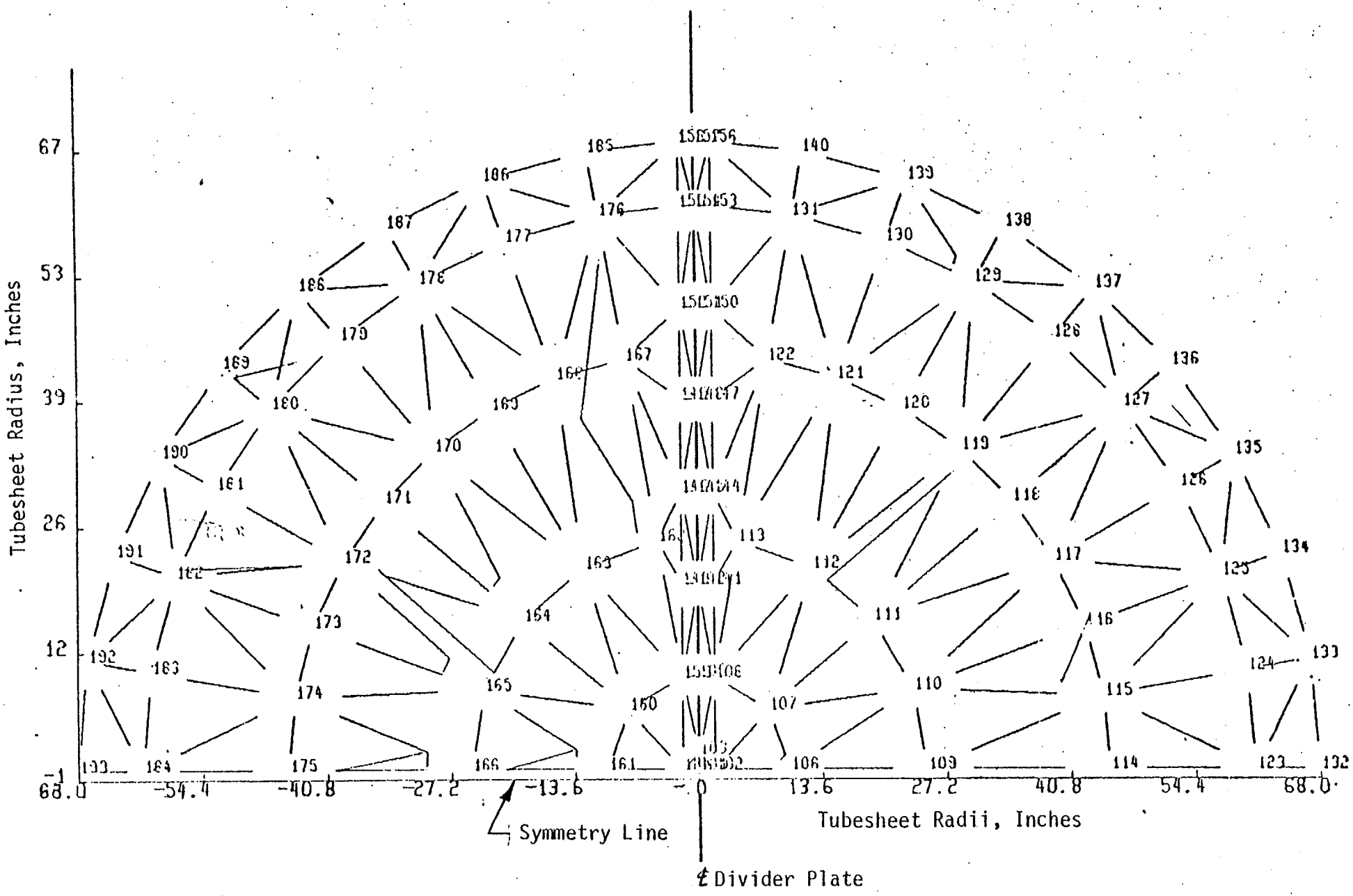

Figure 3.2-9 Node Points, Tubesheet Portion of 3-D ANSYS Model

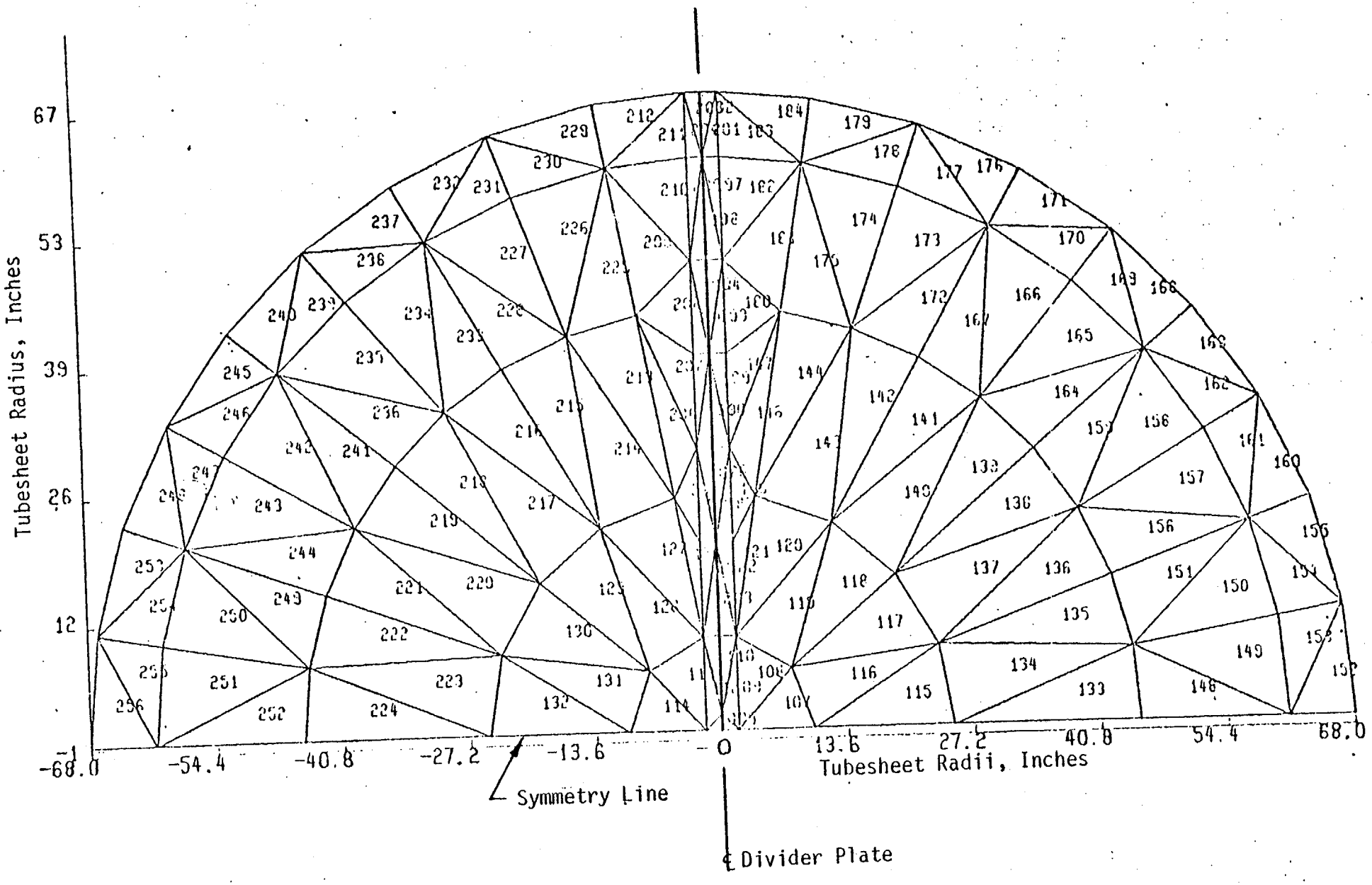

Figure 3.2-10 Elements, Tubesheet Portion of 3-D ANSYS Model

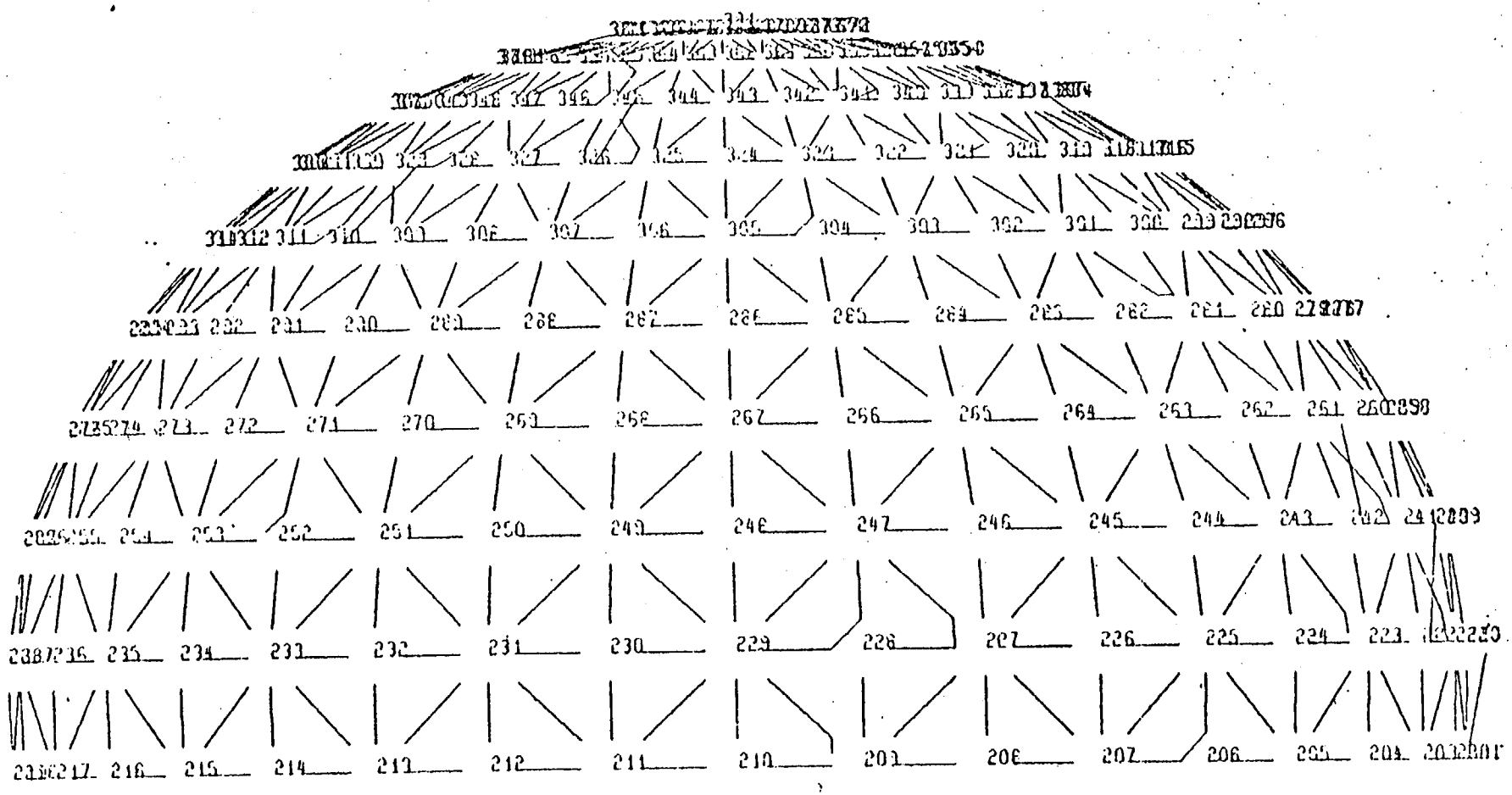

Figure 3.2-11 Node Points, Channel Head Portion of 3-D ANSYS Model

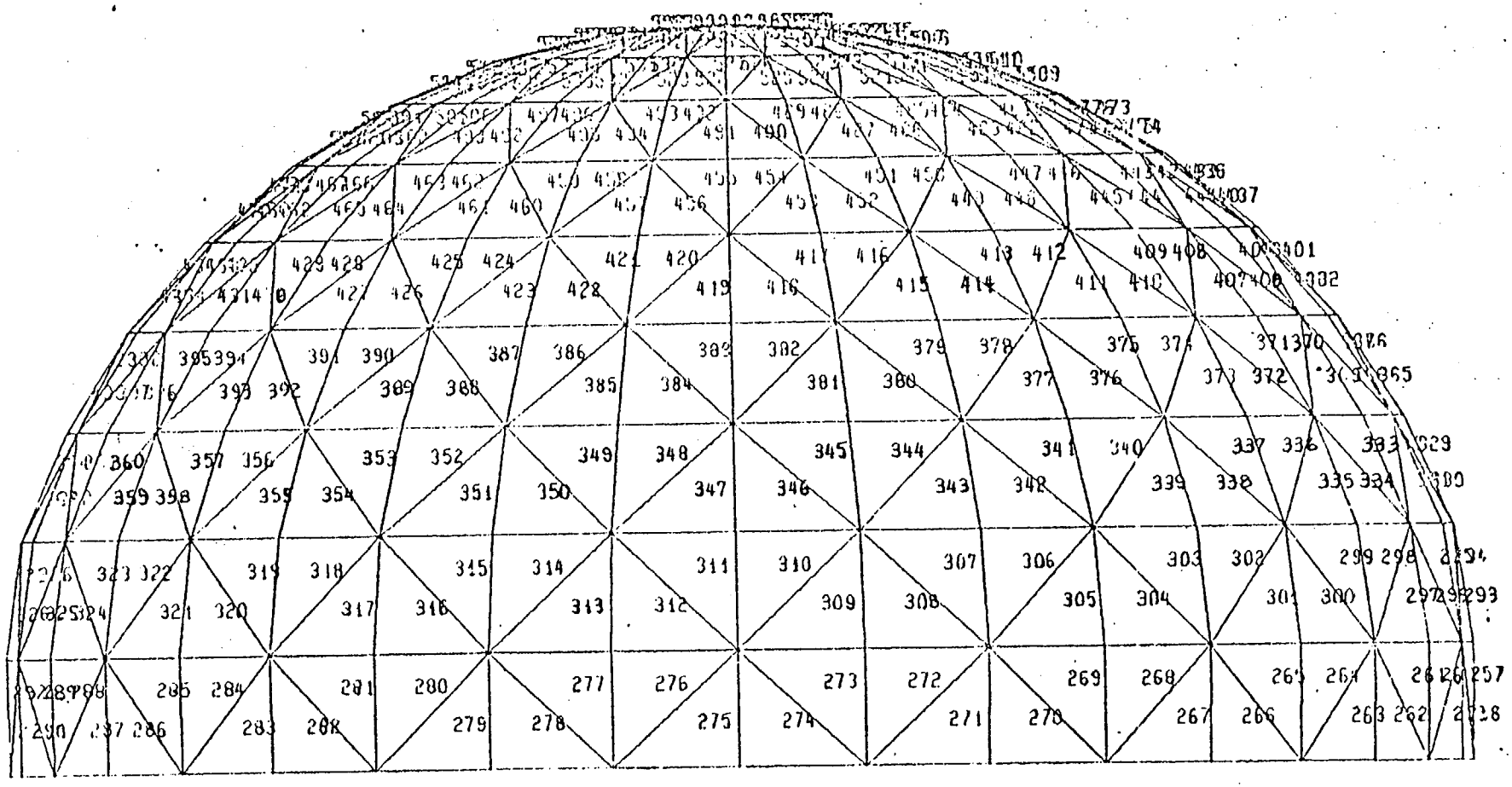

Figure 3.2-12 Elements, Channel Head Portion of 3-D ANSYS Model

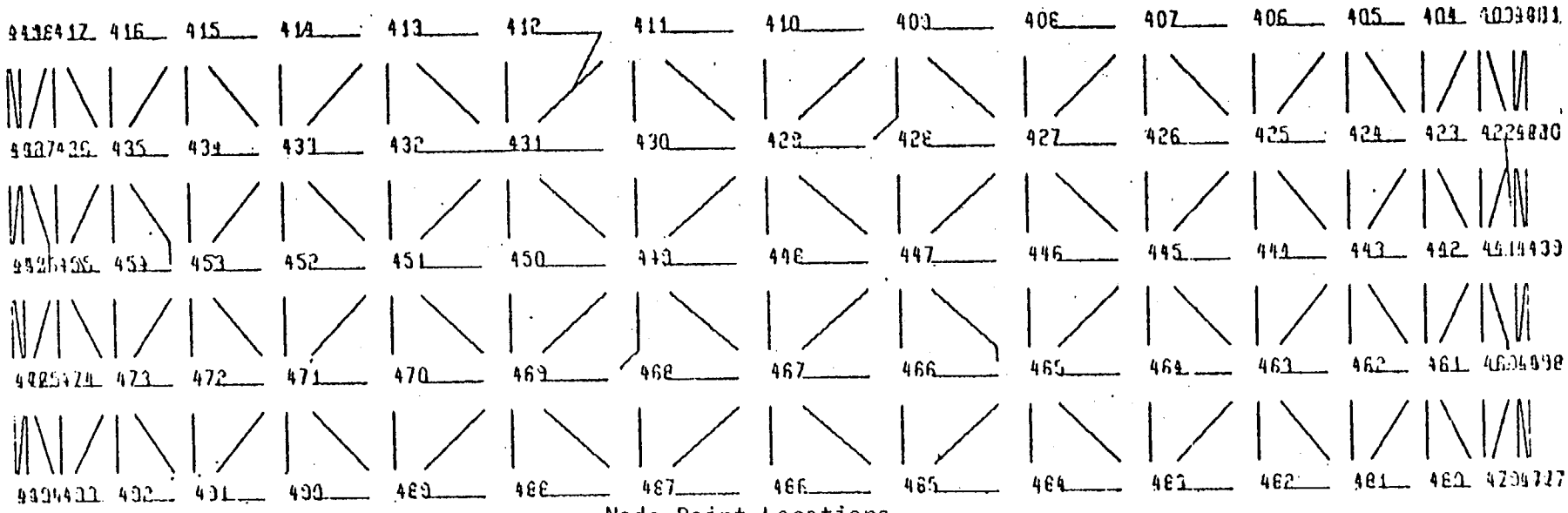

Node Point Locations

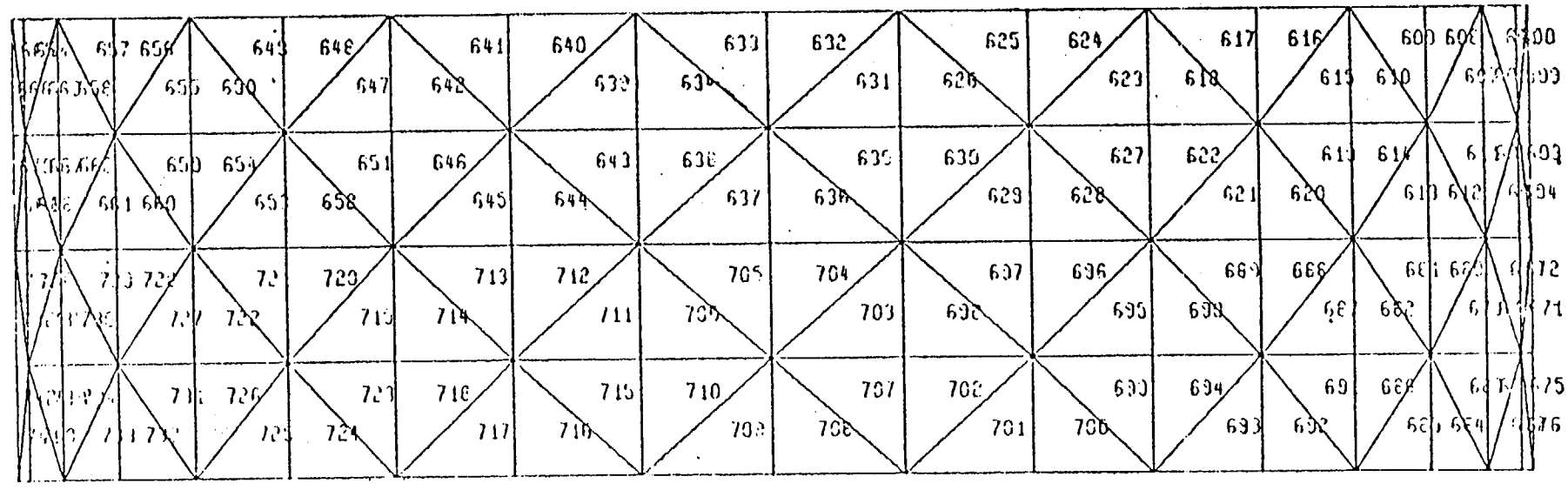

Element Locations

Figure 3.2-13 Stub Barrel Portion of 3-D ANSYS Model

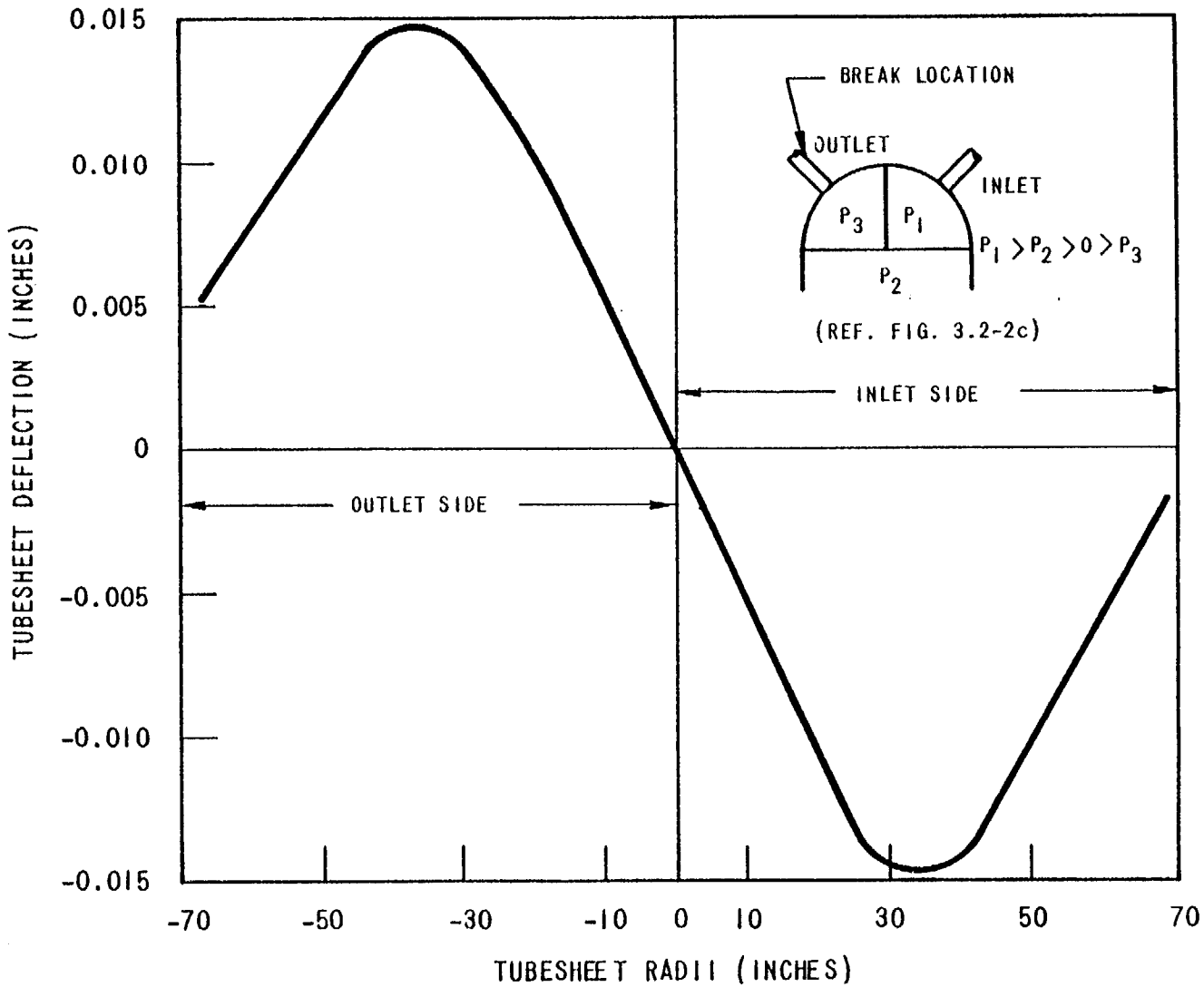

Figure 3.2-14 Tubesheet Deflection Due to LOCA Perpendicular to Divider Plate

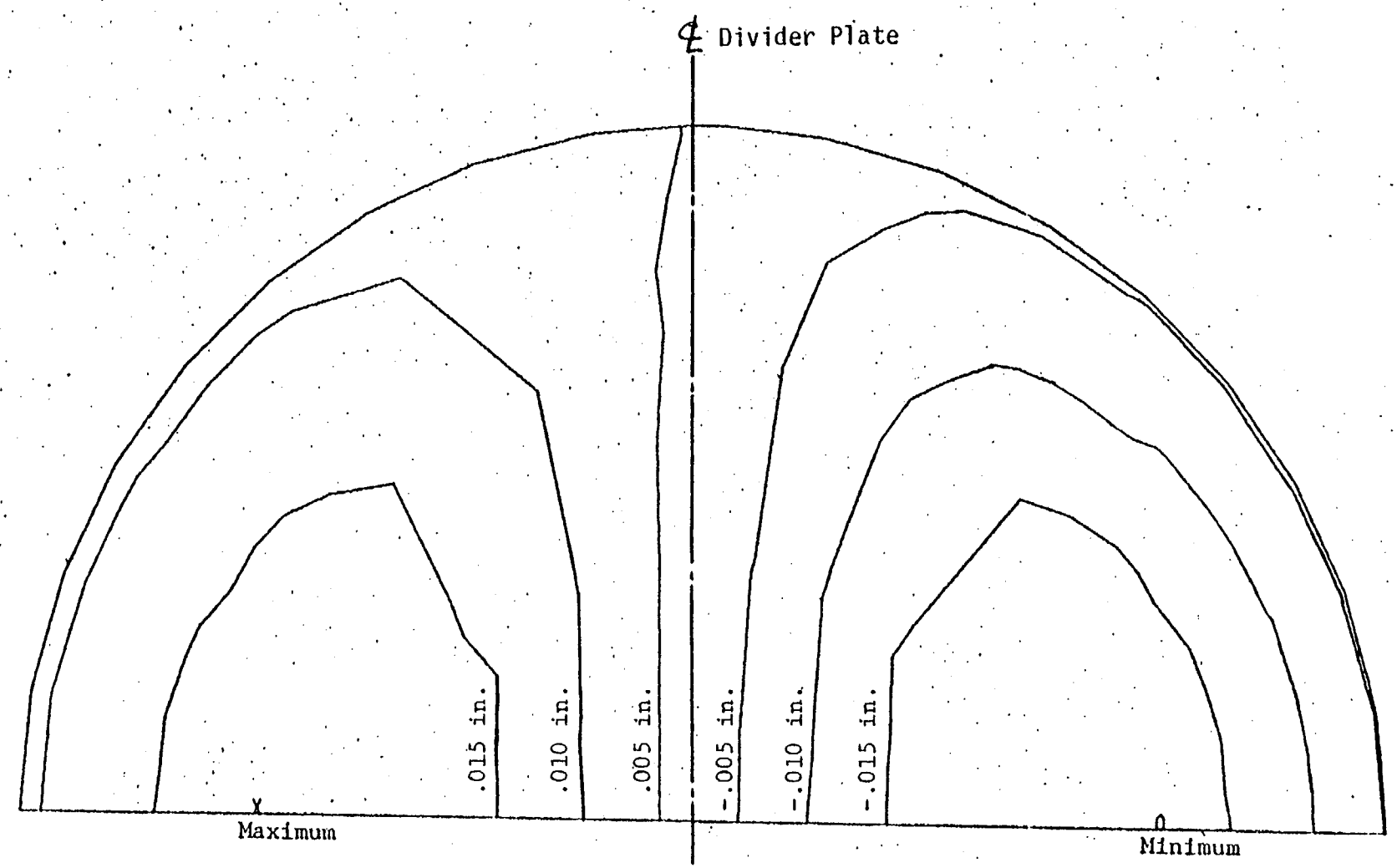

Figure 3.2.-15. Tubesheet Perpendicular Displacement

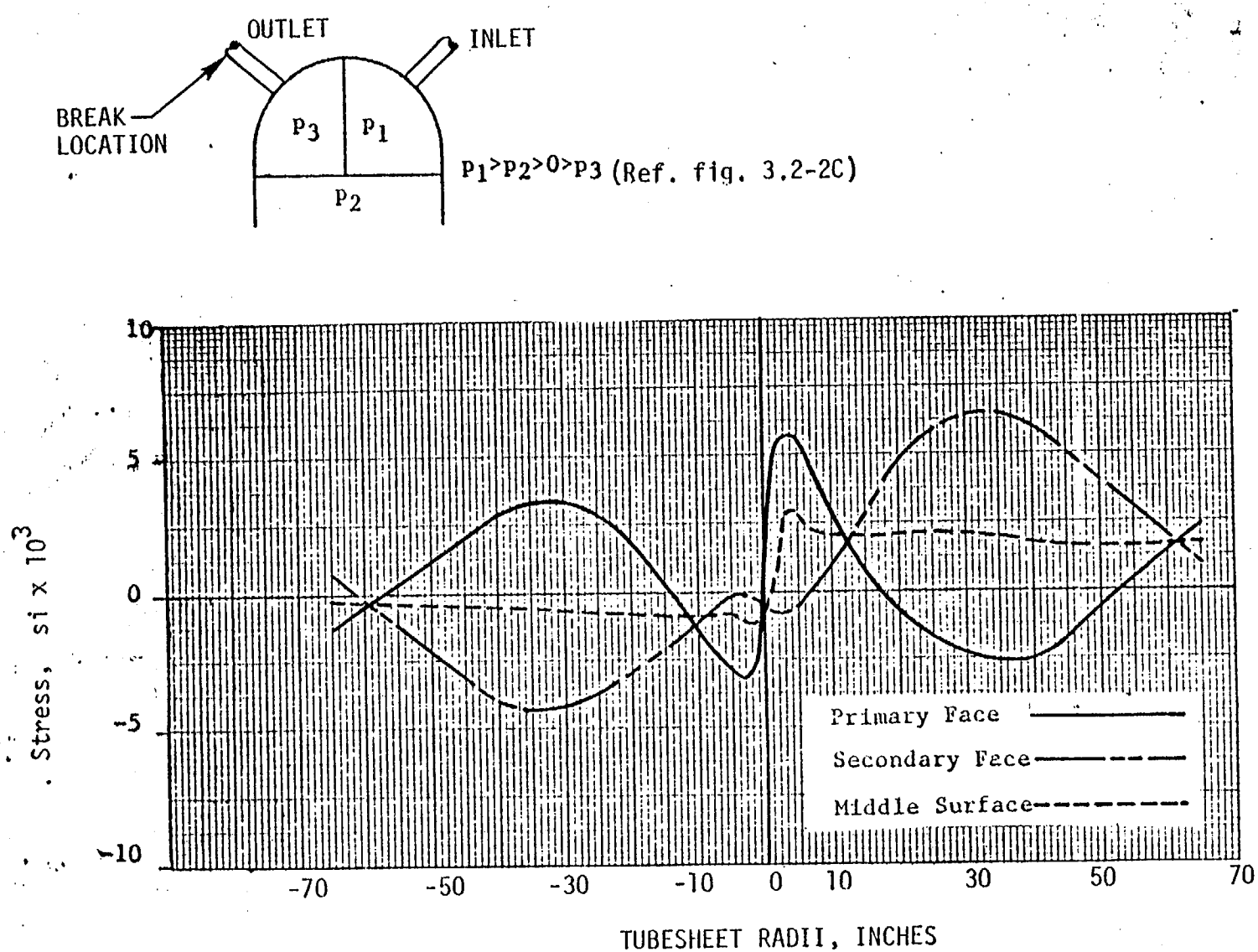

Figure 3.2-16. Tubesheet Equivalent Plate Stresses-Radial Stress Perpendicular to Divider Plate

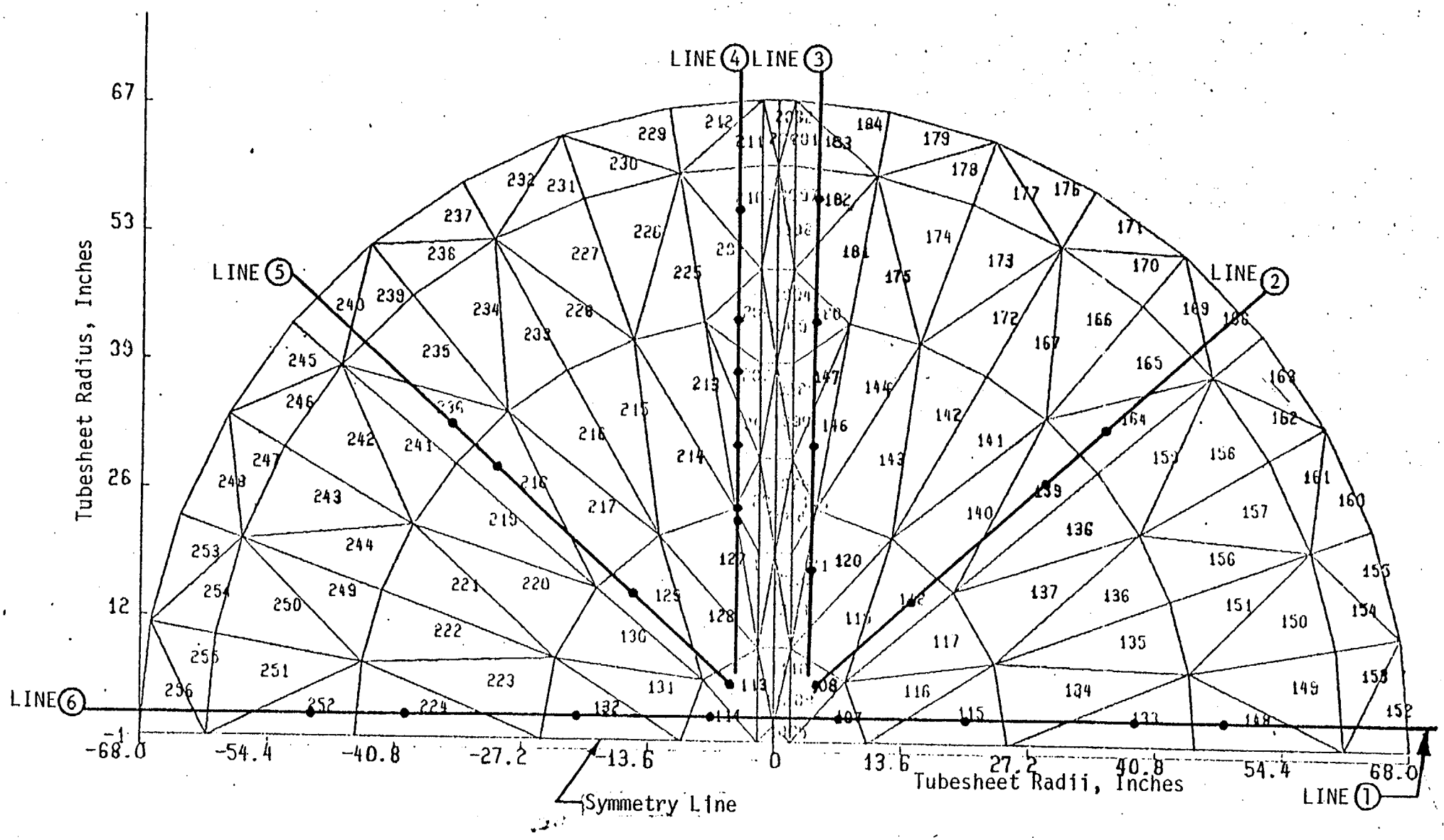

Figure 3.2.-17. Radii on Which Ligament Stresses Were Calculated

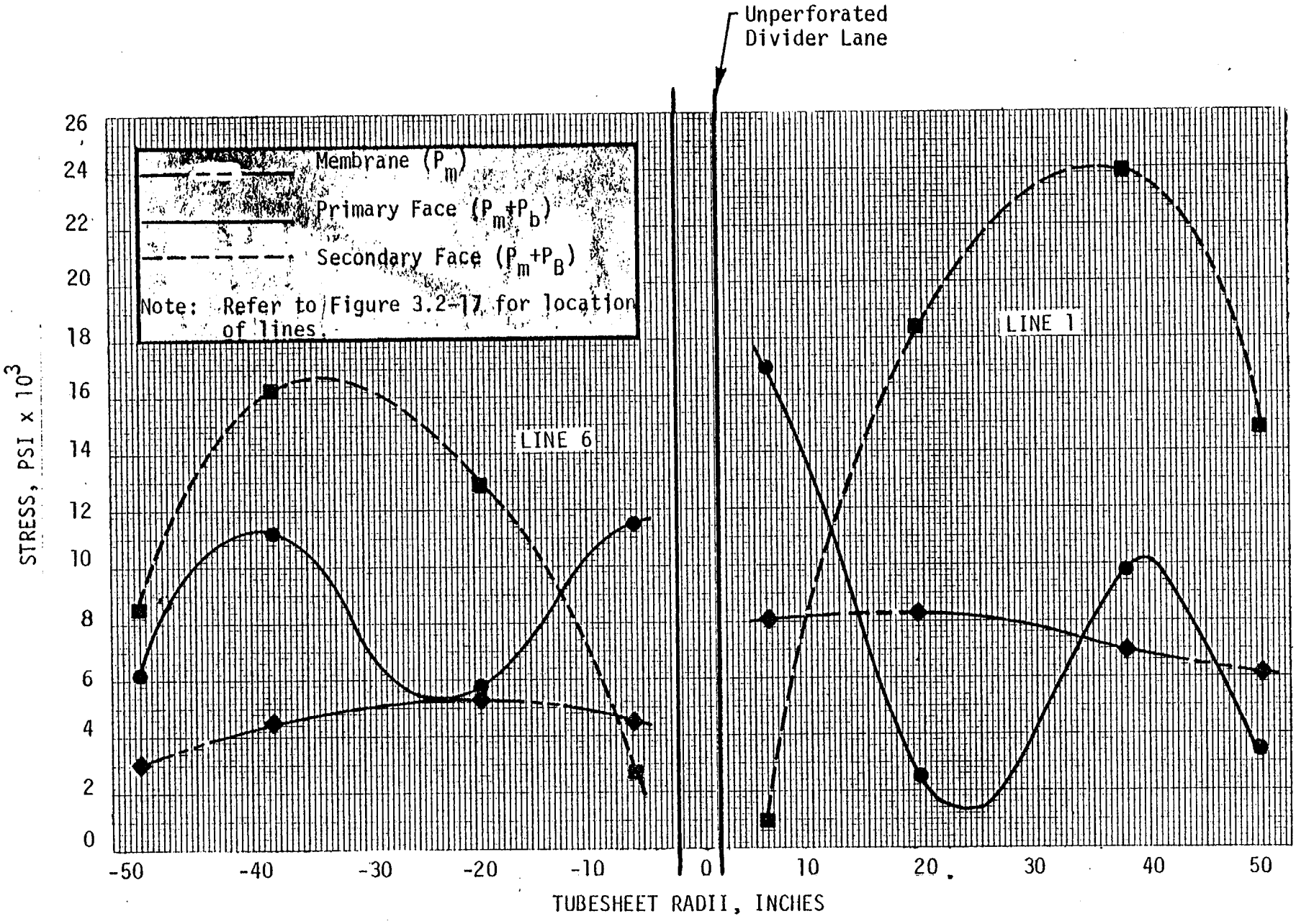

Figure 3.2-18 Ligament Stress Intensities

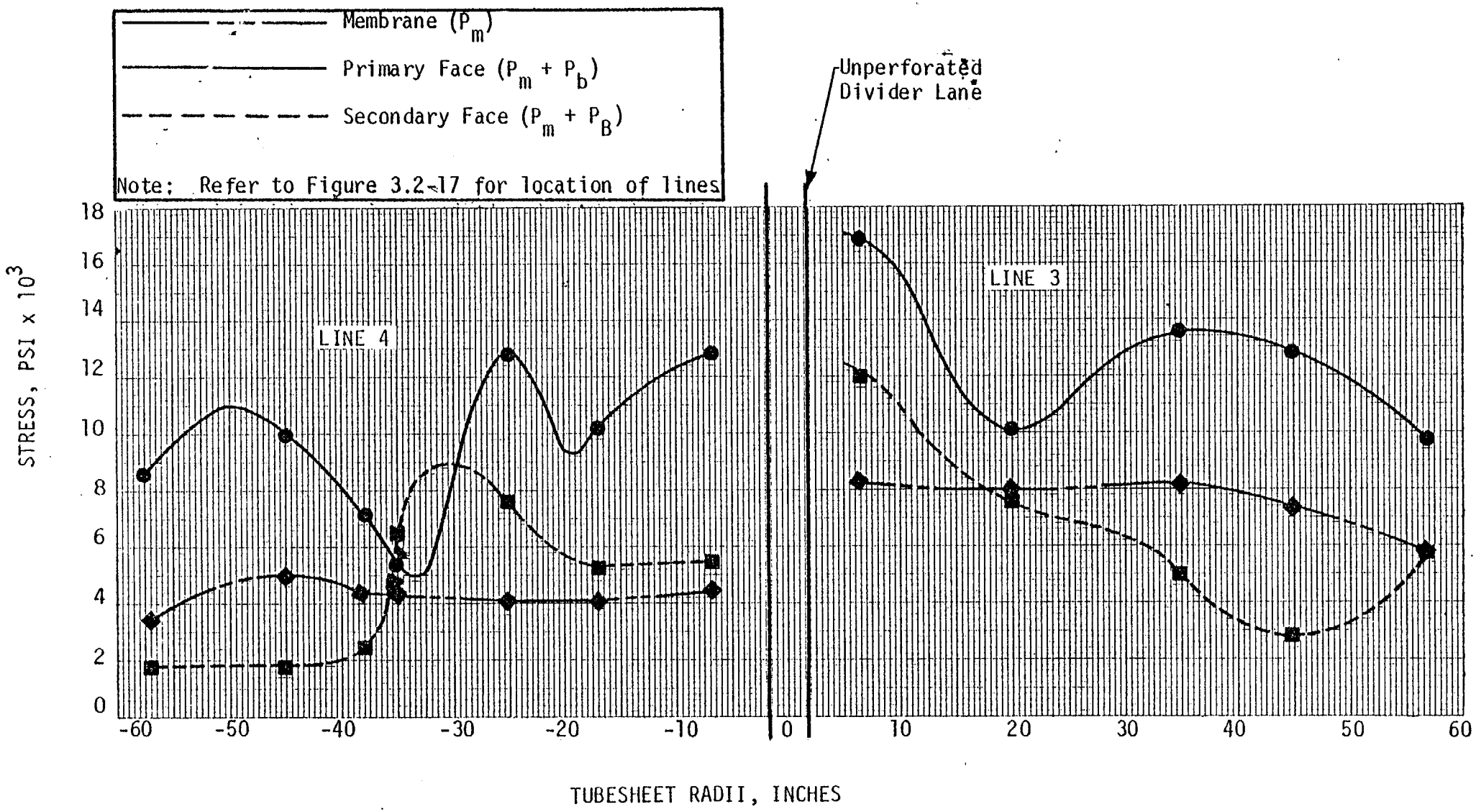

Figure 3.2-19 Ligament Stress Intensities

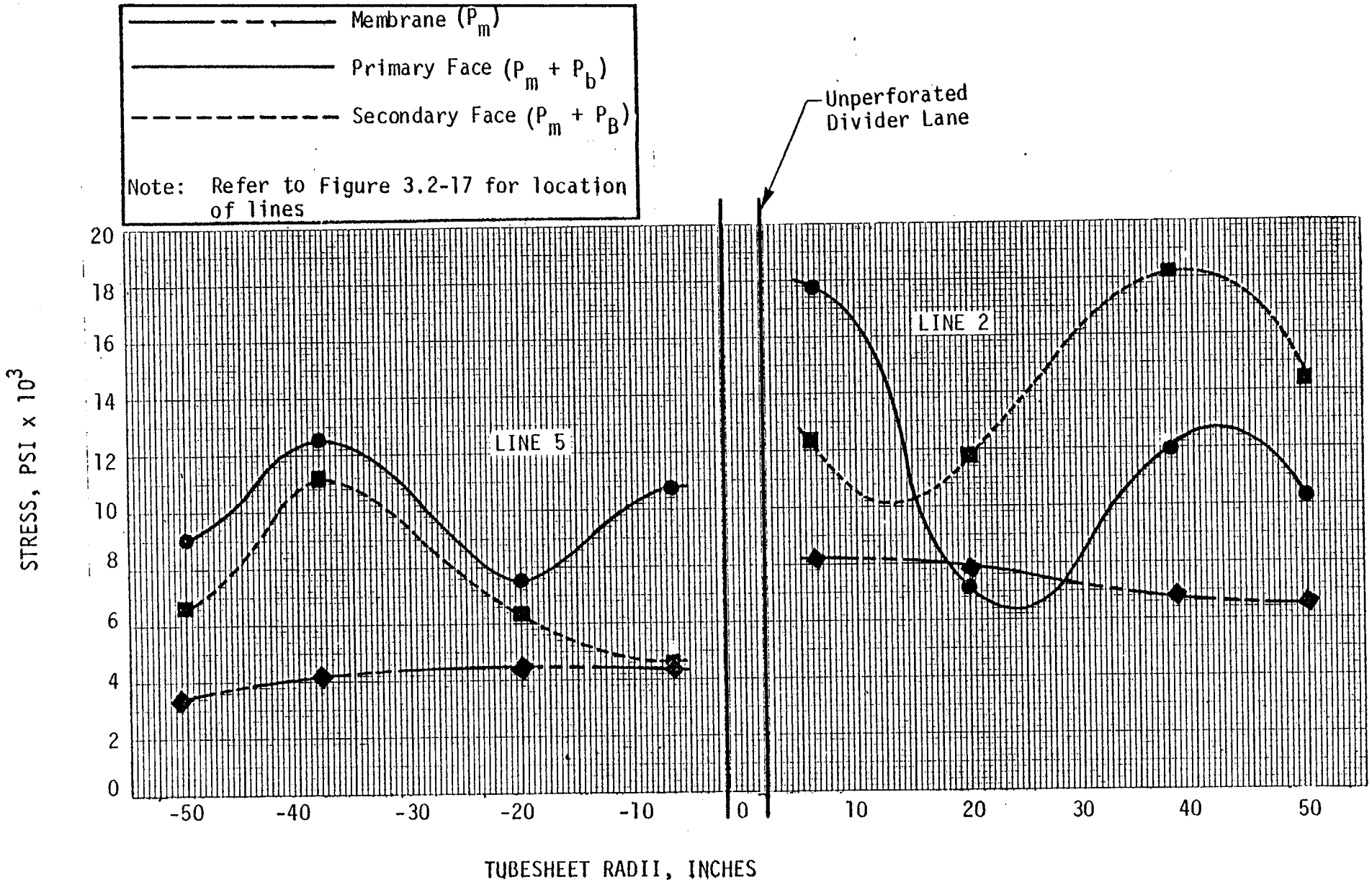

Figure 3.2-20 Ligament Stress Intensities

3.3 DIVIDER PLATE ANALYSIS

This section describes the stress analysis at the Model-D steam generator divider plate during LOCA. In accordance with ASME Code, Section III, the divider plate is not a primary to secondary pressure boundary. However, the structural integrity has been investigated in order to show that no failure will occur resulting in damage to adjacent boundaries.

3.3.1 APPLIED LOAD

The calculated pressure history which was applied as a differential pressure across the divider plate, is shown in Figure 3.3-1. This pressure history was calculated with a modified version of the BLODWN-2 code which accounted for the effect of divider plate flexibility on the hydraulic transient (hydro-elastic effects). As a result, the pressure-history takes into account the change in volume of the steam generator inlet and outlet plenums during deformation of the divider plate. The actual volume change of the plenums, as calculated by the stress analysis, was higher than the calculated volume change in the BLODWN-2 hydro-elastic model. Hence the applied load is conservative. The load used in the analysis (Figure 3.3-2) neglects the perturbations in the calculated load (Figure 3.3-1). Since the amplitudes of the perturbations are substantially less than the maximum load, the gross response of the structure is not affected. The effects of support movement due to LOCA and SSE were neglected, since the tubesheet and channel head complex is very stiff and the resultant forces on the divider plate will be small inertial forces.

3.3.2 STRUCTURAL MODEL

The method of solution for this analysis is based upon computer code W PETROS III B[19,20]. The code is a finite difference program for the calculation of large elastic-plastic dynamically-induced deformation of plates and shells. Figure 3.3-3 illustrates the finite difference mesh along with boundary conditions. The model is structured such that the area containing non-uniform mesh spacing is in a region of low strains.

3.3.3 MATERIAL PROPERTIES

The appropriate material (SB-168) properties are experimental values extracted from Reference [21]. Figure 3.3-4 illustrates the engineering stress-strain characteristics. The S_u value which is used to determine the limit on primary stresses is derived from these curves in accordance with ASME Section III requirements, as follows:

S'_u nominal from curves = 94 KSI

S'_y nominal from curves = 38 KSI

S_y code value = 27.9 KSI

$$S_u = S'_u \times \frac{S_y}{S'_y} = 94 \times \frac{27.9}{38} = 69 \text{ KSI}$$

Figure 3.3-5 is the corresponding true stress-strain data and Figure 3.3-6 is the ~~adjusted~~ true stress-strain curve used in the analysis. Other material properties (at 600°F) used in the analysis are:

$E = 29.2 \times 10^6$ PSI

$\nu = 0.3$

$$\rho = 0.00074 \frac{\text{lb-sec}^2}{\text{in}^4}$$

3.3.4 RESULTS OF ANALYSIS

The limit for primary membrane stresses under faulted conditions is defined as $0.7S_u = 0.7(69) = 48.3$ KSI. The maximum primary membrane stress distribution at the junction of the divider plate to the tubesheet is shown in Figure 3.3-7. The maximum of 27 KSI occurs at the center of the tubesheet and compares well with the limit.

The membrane stress history of the center point of the divider plate is shown in Figure 3.3-8. The maximum stress is 36 KSI and is in the direction

of a parallel to the line of symmetry. This also compares well with the limit. Stresses along the curved edge of the divider plate will be significantly less due to the curvature.

The divider plate attains a maximum displacement of 7.4 inches after 40 msec. into the applied transient loading (See Figure 3.3-9). Since the maximum pressure occurs at 32 msec., this indicates that there is some dynamic effect. The displacement contours at 40 msec. are shown in Figure 3.3-10.

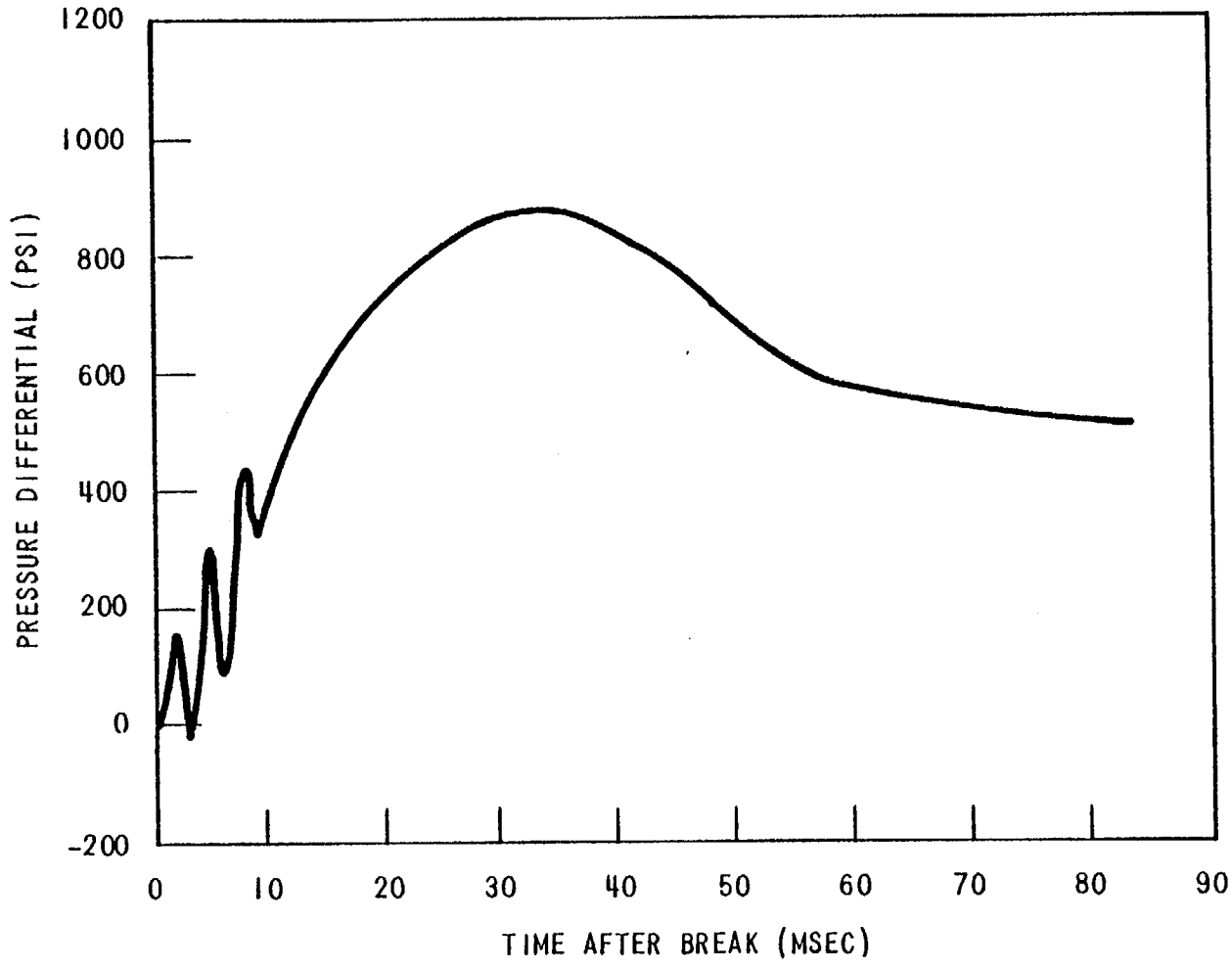

FIGURE 3.3-1 Pressure Difference Across Divider Plate

6899-5

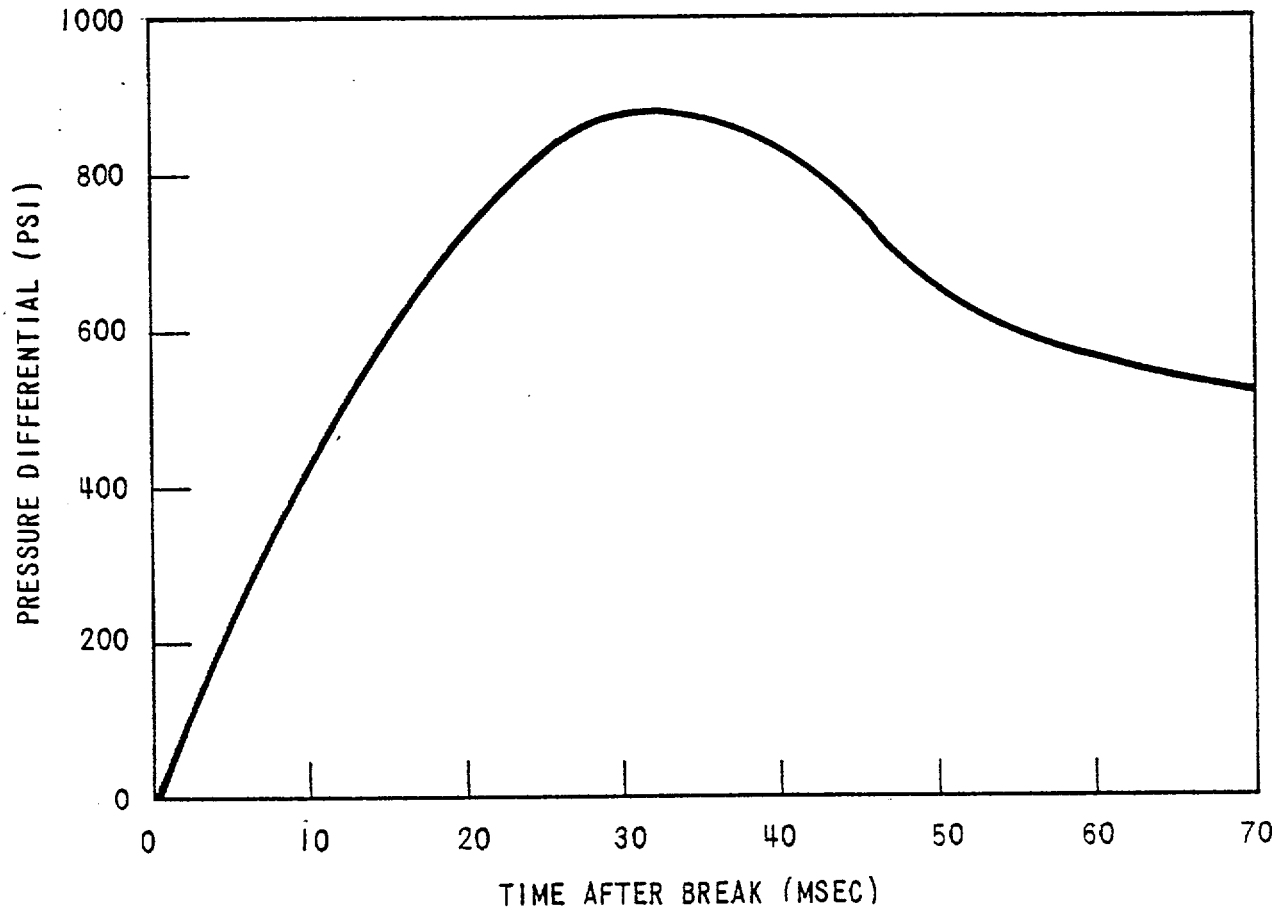

FIGURE 3.3-2 Smoothed Pressure History Across Divider Plate

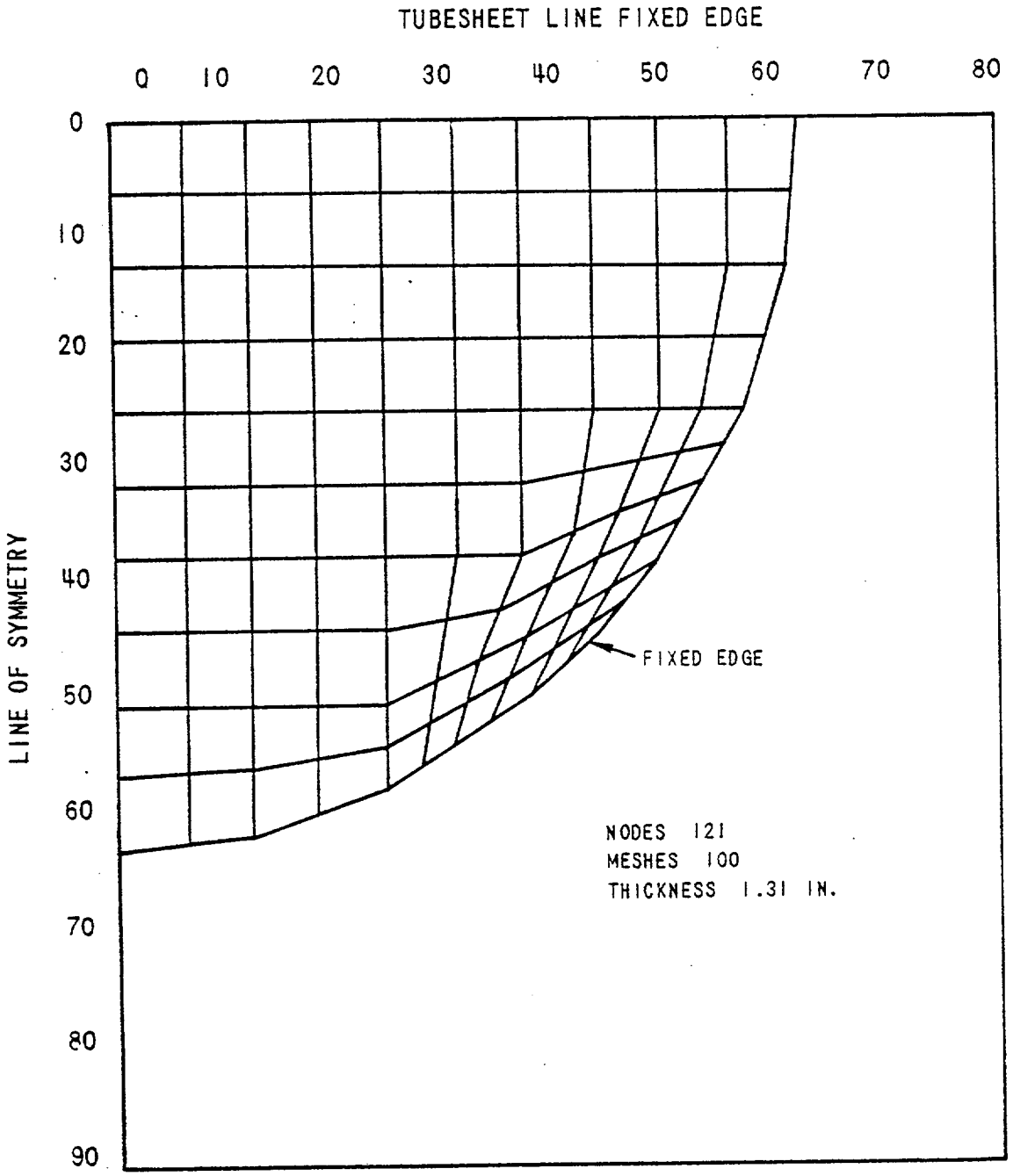

FIGURE 3.3-3 Divider Plate - Finite Difference Mesh Model

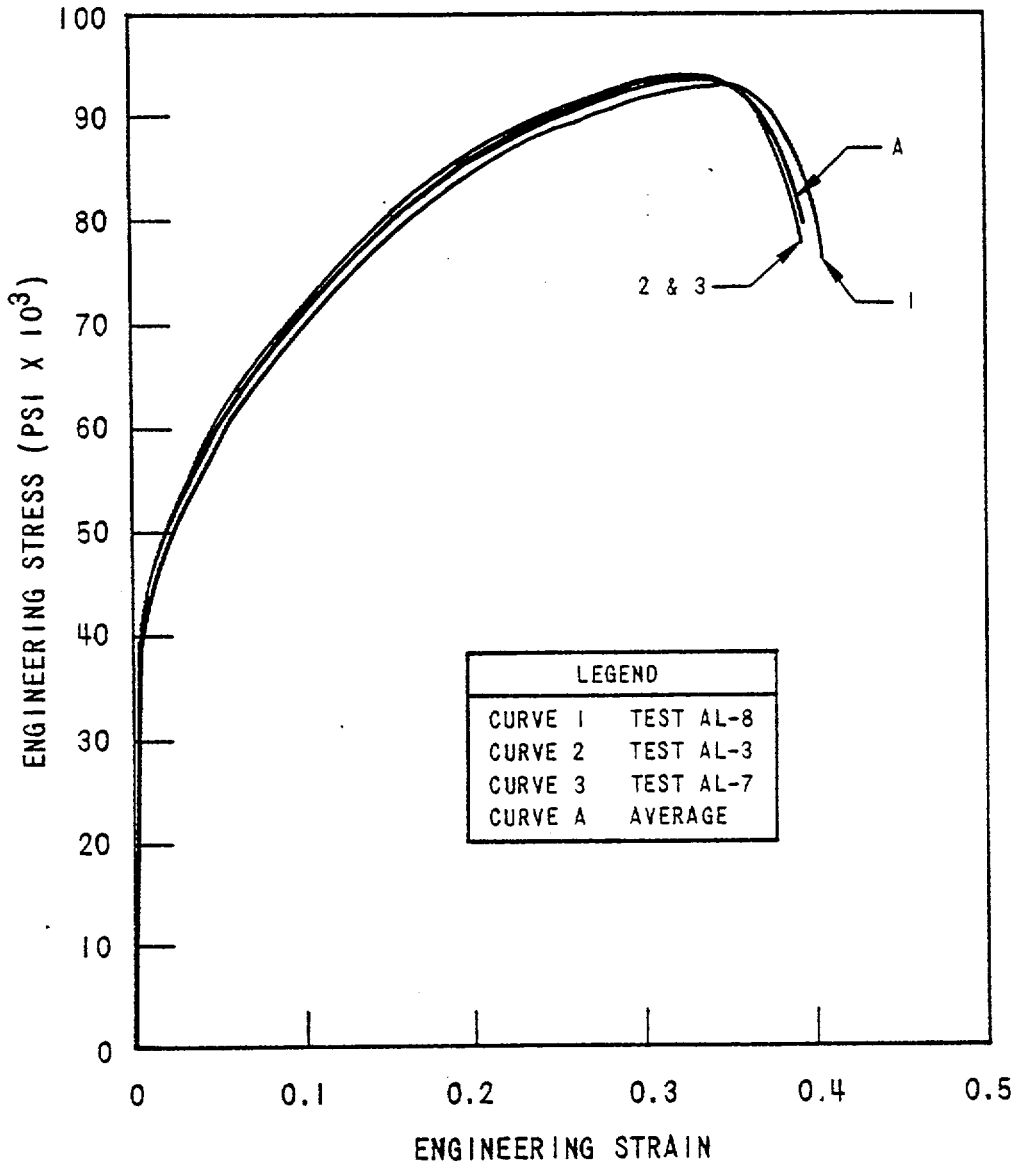

FIGURE 3.3-4 Engineering Stress-Strain Curves for Inconel at 600°F

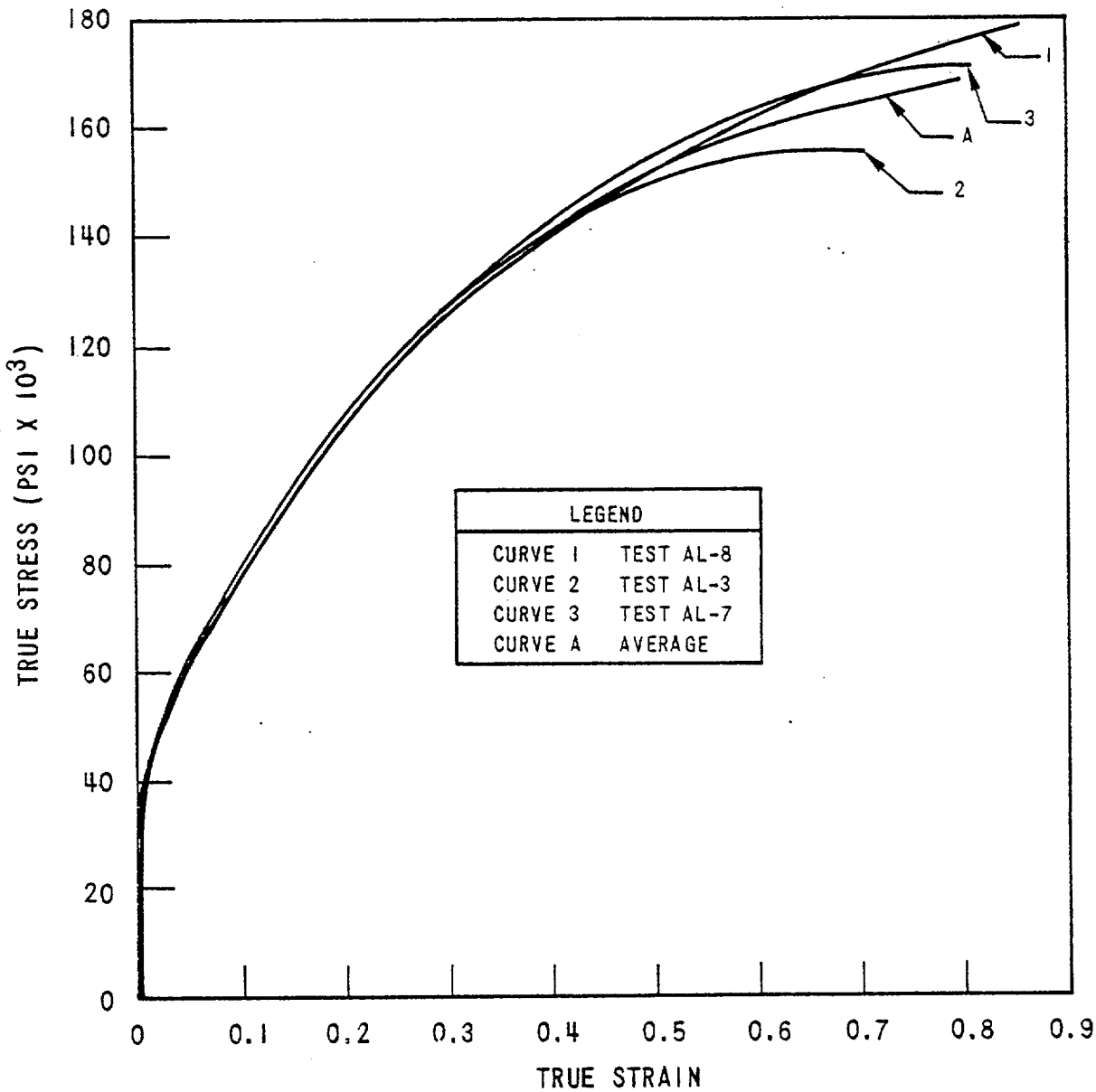

FIGURE 3.3-5 True Stress-Strain Curve for Inconel at 600°F

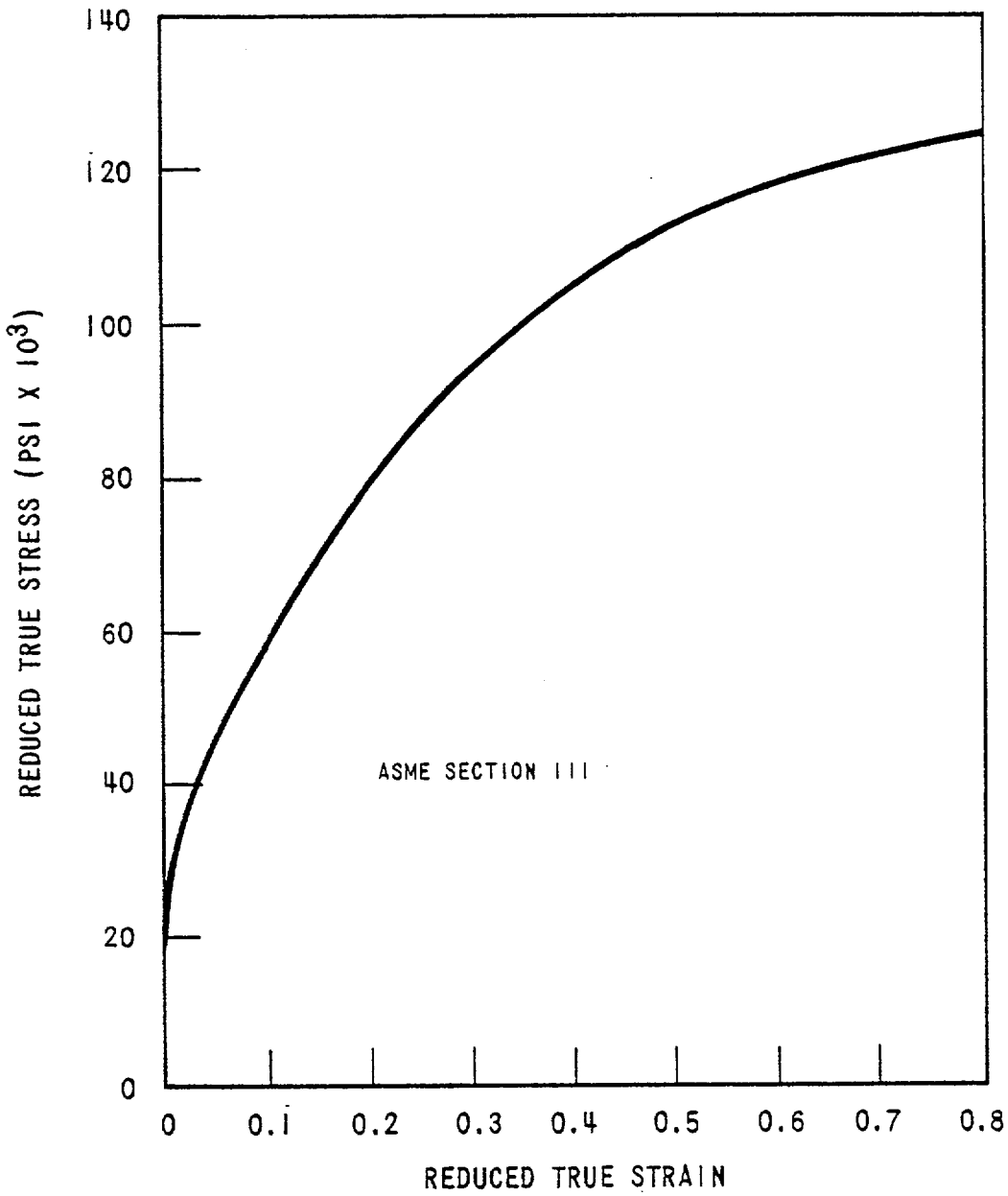

FIGURE 3.3-6 Reduced True Stress - Strain Curve for Inconel at 600°F

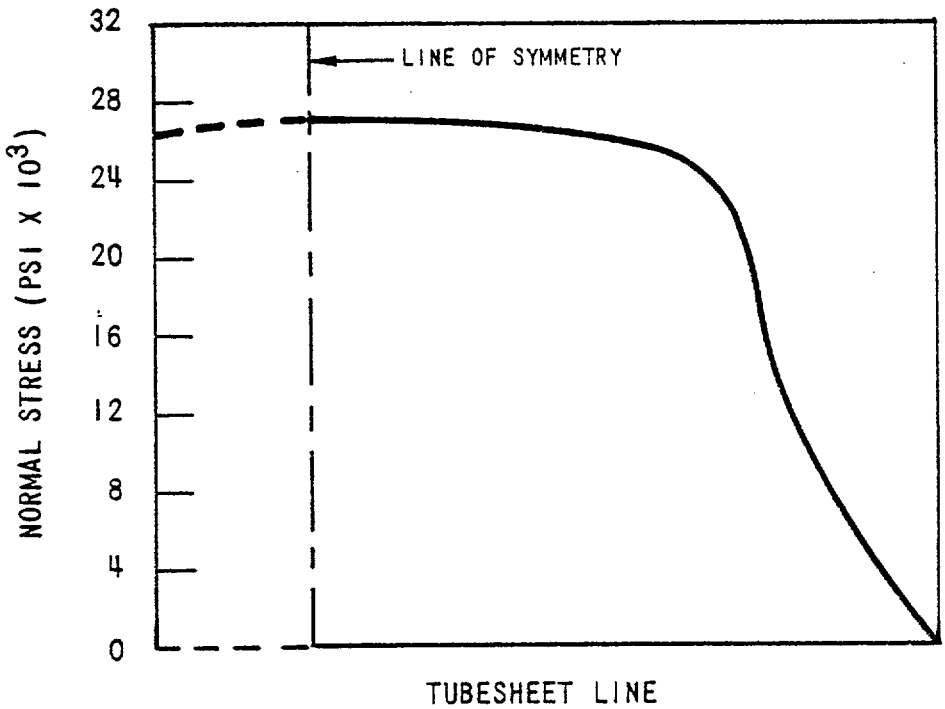

FIGURE 3.3-7 Maximum Membrane Stress at Tubesheet Line

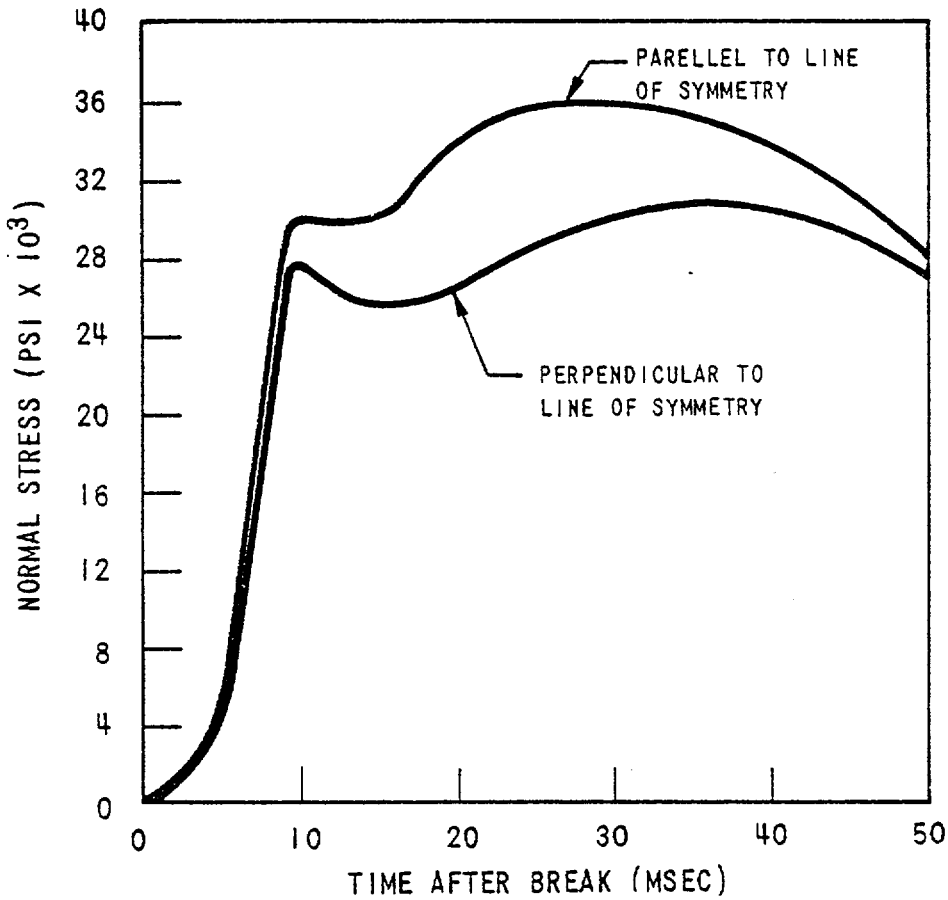

FIGURE 3.3-8 Membrane Stress History at Point of Maximum Deflection on Divider Plate

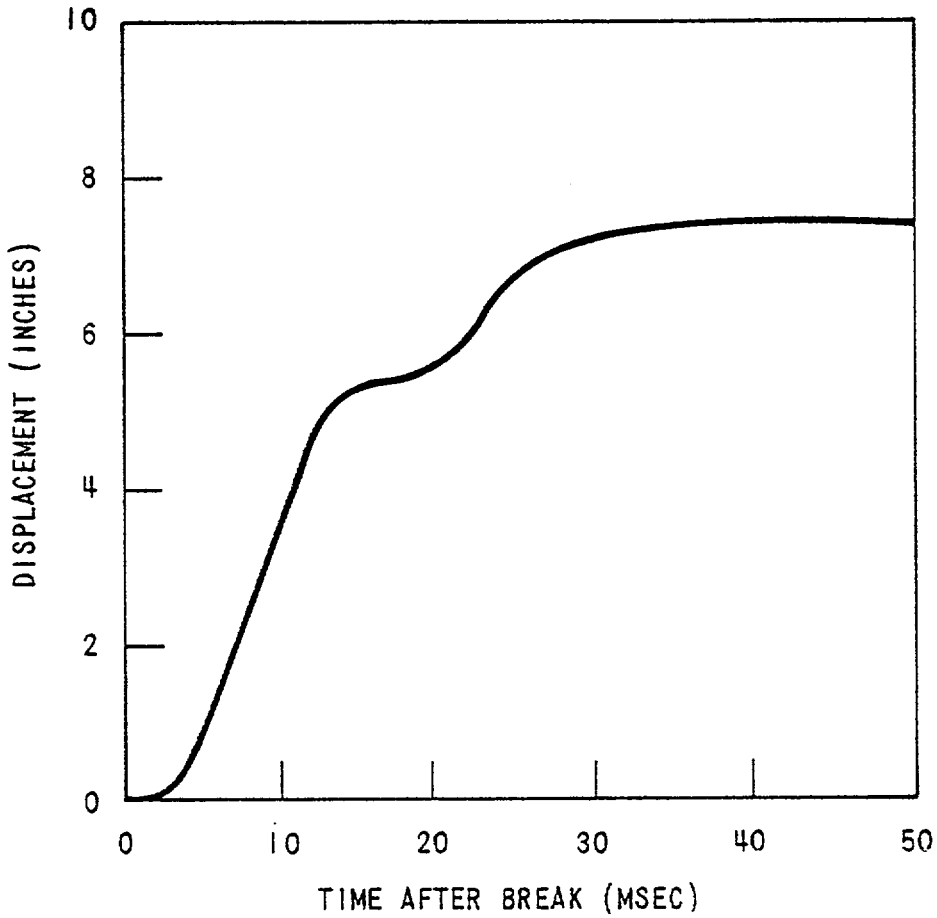

FIGURE 3.3-9 Displacement History of Point of Maximum Deflection, in the Center of the Divider Plate

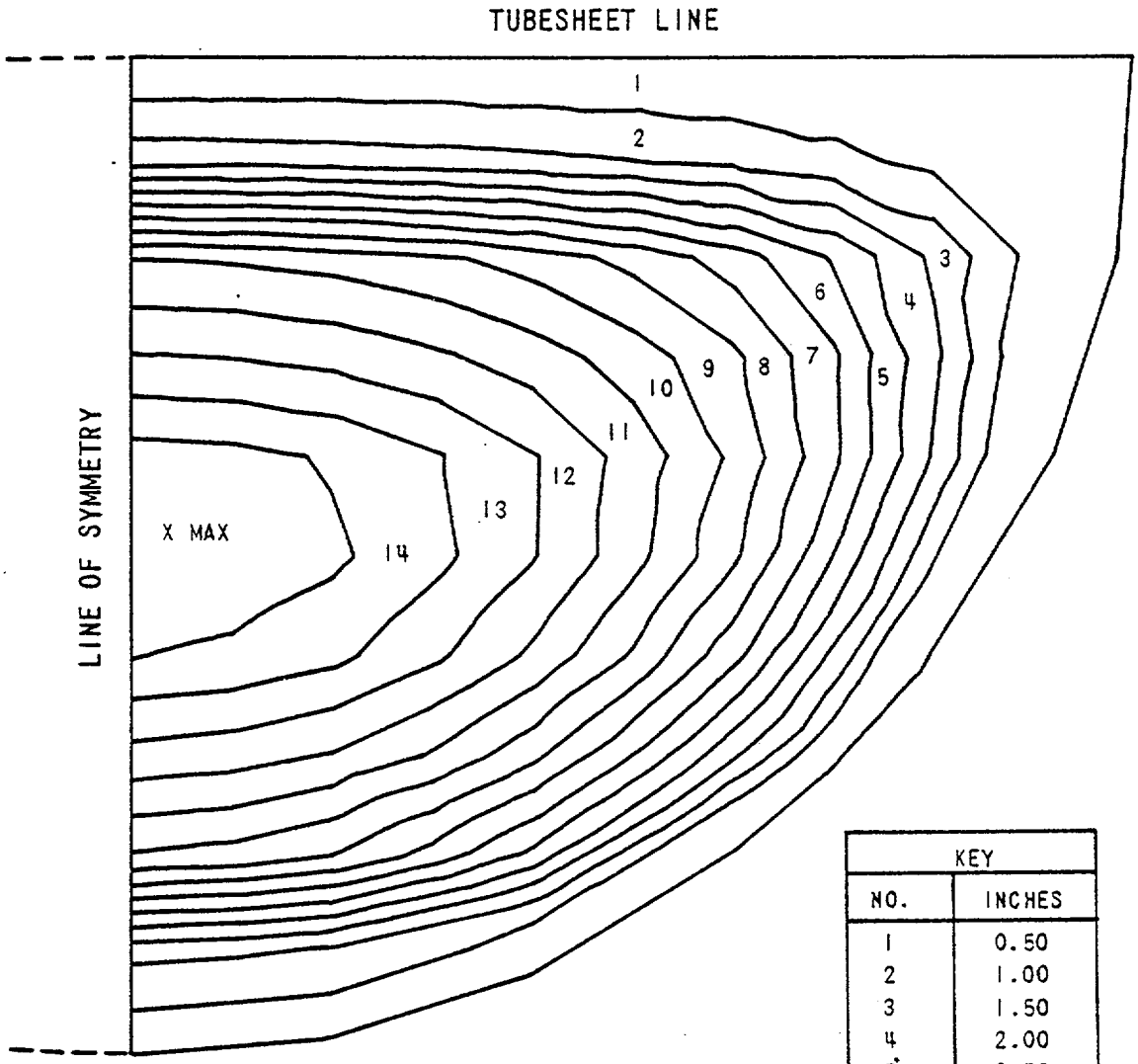

KEY	
NO.	INCHES
1	0.50
2	1.00
3	1.50
4	2.00
5	2.50
6	3.00
7	3.50
8	4.00
9	4.50
10	5.00
11	5.50
12	6.00
13	6.50
14	7.00

FIGURE 3.3-10 Displacement Contours at Maximum Pressure Differential, For Divider Plate

4.0 CONCLUSIONS

The structural integrity of the tubes, divider plate, and tubesheet of current Westinghouse steam generators is assured during a Loss of Coolant Accident at the steam generator coolant outlet nozzle in combination with a Safe Shutdown Earthquake. The criteria used to evaluate these components under this Faulted Condition are those of the 1971 ASME Section III Code, Appendix F. In addition, this study establishes the minimum allowable tube wall which can sustain these conditions (.026 in wall, for the model D) and that the critical flow size on a Model D tube after forty years life (0.036 in wall) is 0.64 ins.

The following is a summary of maximum calculated stresses in the components, compared with the code allowable limits.

Component	Stress Category	Maximum Calculated Stress Intensity (KSI)	Section III Limit (KSI)
TUBE (.036 in wall)	P_m	16.79	52.5
	$P_m + P_B$	55.0	78.75
THINNED TUBE (.026 in wall)	P_m	23.0	52.5
	$P_m + P_B$	75.1	78.75
TUBESHEET	P_m	8.32	56.0
	$P_m + P_B$	25.2	84.0
DIVIDER PLATE	P_m	36.0	48.3

The calculated collapse pressure for the .036 in. wall tube at 600°F is approximately 3000 psi for 0% ovality and 1830 psi for the maximum allowable 5% ovality. These are higher than the maximum expected secondary side pressure minus containment back pressure.

5.0 REFERENCES

1. Fabic, S. "Description of the BLODWN-2 Computer Code," WCAP-7918, October, 1970.

2. Bordelon, F. M. "A Comprehensive Space-Time Dependent Analysis of Loss-of-Coolant (SATAN-4 Digital Code)", WCAP-7750, August, 1971.

3. Fabic, S. "Loss-of-Coolant Analysis: Comparison between BLODWN-2 Code Results and Test Data", WCAP-7401, November, 1969.

4. Moore, J. S. "Westinghouse PWR Core Behavior Following a Loss-of-Coolant Accident", WCAP-7422, August, 1971.

5. Dingwell, I. W., Bradshaw, R. T. "Static, Thermal, Dynamic Pipe Stress Analysis Operating Manual", Arthur D. Little, Inc.

6. Greenstadt, J. "The Determination of the Characteristic Roots of a Matrix by the Jacobi Method," in "Mathematical Methods for Digital Computers," edited by Anthony Ralston, Chapter 7, pp. 84-91, Whiley, New York, 1960.

7. "Reference Safety Analysis Report", RESAR-41, Westinghouse Nuclear Energy Systems, December 1973, Chapter 5, pp. 5.2-38 - 5.2-42.

8. Smith, P. G. "Earthquake Analysis of Structures by the Response Spectrum Method," WCAP-7648, February 1971.

9. STASYS-2 User's Manual WCAP-7651, Westinghouse Electric Corporation, March 1971.

10. ASME Boiler and Pressure Vessel Code Section III, Nuclear Power Plant Components, 1971 Edition.

11. "Rules for the Evaluation of Faulted Conditions", Proposed Appendix F of the ASME Section III Code.

12. ASME Code Case 1484.

13. Roark, R. J., "Formulas for Stress and Strain," McGraw-Hill Book Company.

14. Eiber, R. J. et al, "Investigation of the Initiation and Extent of Ductile Pipe Rupture," BMI-1866, Battelle Memorial Institute, July 1969.

15. Flugge, W., Handbook of Engineering Mechanics, 1962.

16. Swanson, J. A., "Engineering Analysis System (ANSYS) User's Manual," Swanson Analysis Systems, Inc. 1971.

17. O'Donnell, W. J., "A Study of Perforated Plates with Square Penetration Patterns," WRC Bulletin #124 September, 1967.

18. Timoshenko, S. P. and Woinowsky-Kreiger, S., "Theory of Plates and Shells", McGraw-Hill, 1959, p. 57.

19. Atluri S., Witmer, E. A., Leech, J. W., Morino, L., "PETROS III A Finite Difference Method and Program for the Calculation of Large Elastic-Plastic Dynamically - Induced Deformation of Multilayer Variable - Thickness Shells", MIT, ASRL TR 152-2, November, 1971.

20. Rinne, W. A., "Explanatory Manual for Utilization of the W PETROS 3B Computer Code", WTD-ASM-73-025, November 1973.

21. Iorio, N., "Tensile Properties of PWR Materials", TD-MET-73-054, 1973.

APPENDIX A

ADDITIONAL INFORMATION

UNITED STATES
ATOMIC ENERGY COMMISSION
WASHINGTON, D.C. 20545

AUG 12 1974

Mr. Romano Salvatori, Manager
Nuclear Safety Department
Westinghouse Electric Corporation
P. O. Box 355
Pittsburgh, Pennsylvania 15230

Dear Mr. Salvatori:

In order that we may complete our review of Westinghouse Electric Corporation topical report WCAP-7832 (Non-proprietary) entitled "Evaluation of Steam Generator Tube, Tube Sheet and Divider Plate Under Combined LOCA Plus SSE Conditions," additional information is required. Enclosure 1 identifies the required information.

After the requested information has been received, a schedule for completion of review of WCAP-7832 will be established.

If you have any questions concerning our request for additional information, please contact us.

Sincerely,

D. B. Vassallo, Chief
Light Water Reactors Project Branch 1-1
Directorate of Licensing

Enclosure:
Request for Additional
Information on WCAP-7832

RECEIVED
AUG 19 1974

R. SALVATORI

MECHANICAL ENGINEERING BRANCH

DIRECTORATE OF LICENSING

REQUEST FOR ADDITIONAL INFORMATION

TOPICAL REPORT: WCAP-7832

EVALUATION OF STEAM GENERATOR TUBE, TUBE SHEET AND DIVIDER PLATE UNDER COMBINED LOCA PLUS SEE CONDITIONS

1. The steam generator described in RESAR-3 contains a preheater section consisting of a baffle plate and tube support plates attached to the baffle and to the steam generator shell. In Section 2.3 of WCAP-7832 this sub-structure is apparently not included in the seismic model of the steam generator. Discuss the effect of this structure on the response of this model

2. In Section 3.1

A. a. Provide a description of the computer program STACYS used in the tube analysis.

b. Provide the basis for the assumed 40 year tube thinning.

c. Provide a reference or additional data on crack propagation tests on tubes loaded by combined internal pressure and axial bending moments.

d. Provide a reference or additional data on the tube collapse tests, and the analytical correlation and analysis on which the extrapolation of test results to tubes of different yield strength and wall thickness is based.

B. a. Describe the analyses employed to assess the effect of a postulated steam line break on the steam generator tubes and provide a summary of the results.

b. Describe the analyses employed to assess the effect of a postulated break at the feedwater nozzle on the preheater substructure and provide a summary of the results.

c. Discuss the effects of local thinning due to wear and local crud accumulation at the tube supports on the burst strength of the tubes.

d. Identify the method by which corrosion phenomena were considered in assessing the fatigue strength of the tubes.

3. a. Provide justification for using different pressure-time histories in the tube sheet analysis and the divider plate analysis.

b. Provide a comparison of the maximum deflection and stress in the divider plate as calculated from ANSYS and PETROS.

October 31, 1974
NS-RS-453

Mr. D. B. Vassallo, Chief
Light Water Reactors Project Branch 1-1
Directorate of Licensing
United States Atomic Energy Commission
Washington, D.C. 20545

Dear Mr. Vassallo:

Enclosed are 15 copies of the additional information requested in your letter of August 12, 1974 in order to complete your review of Westinghouse Electric Corporation topical report WCAP-7832 (non-proprietary) entitled "Evaluation of Steam Generator Tube, Tubesheet and Divider Plate under Combined LOCA Plus SSE Conditions."

WCAP-7832 presented an analysis of the steam generator structural integrity to demonstrate its capability to sustain stresses resulting from simultaneous LOCA and SSE loading conditions. Detailed discussion and analysis of other postulated chemical, metallurgical or mechanical considerations during operation are beyond the scope of this report, but may be referred to in the individual SAR's. However, for purposes of additional clarification responses to questions 2Ac, 2Ad, 2Ba, 2Bb, and 2Bc of your August 12, 1974 letter have been included in the attachment.

We request review of the attached information and establishment of a schedule for the completion of review of WCAP-7832.

We request consideration of WCAP-7832 and the additional information of the attachment in conjunction with future safety analysis report references.

Sincerely yours,

R. Salvatori, Manager
Nuclear Safety Department

clc

Attachment

cc ~~RMA~~
JE~~MC~~

UNITED STATES
NUCLEAR REGULATORY COMMISSION
WASHINGTON, D. C. 20555

NOV 12 1975

Mr. C. Eicheldinger, Manager
Nuclear Safety Department
Westinghouse Electric Corporation
P. O. Box 355
Pittsburgh, Pennsylvania 15230

RECEIVED
NOV 17 1975
C. EICHELDINGER
PWR NUCLEAR SAFETY

Dear Mr. Eicheldinger:

To complete our review of Westinghouse Electric Corporation report WCAP-7832 (Non-proprietary) entitled, "Evaluation of Steam Generator Tube, Tube Sheet and Divider Plate Under Combined LOCA Plus SSE Conditions", additional information is required. The required information is identified in Enclosure 1.

To meet our review schedule, we need this additional information by December 19, 1975. If you cannot meet this schedule, please inform us within ten days after receipt of this letter of the date you plan to submit your response.

If you have any questions about our request for additional information, please contact us.

Sincerely,

D. B. Vassallo, Chief
Light Water Reactors
Project Branch 1-1
Division of Reactor Licensing

Enclosure:
Request for Additional
Information

NOV 12 1975

ENCLOSURE 1

MECHANICAL ENGINEERING BRANCH

OFFICE OF NUCLEAR REACTOR REGULATION

REQUEST FOR ADDITIONAL INFORMATION

WESTINGHOUSE REPORT: WCAP-7832

EVALUATION OF STEAM GENERATOR TUBE, TUBE SHEET AND DIVIDER PLATE UNDER COMBINED LOCA PLUS SSE CONDITIONS

1. Regarding your reply to Item 2.B.d of our request for additional information, dated August 12, 1974, explain the increase in strength of service exposed tubes with no intergranular corrosion as compared with tubes of origin material, as shown in Figure VII -5 (p. 24d) of your reply.

2. (a) Define the term "stress intensity."

   (b) Show that the maximum "membrane plus bending" stress intensities in healthy and thinned tubes are lower than the allowable stress limits when effects due to normal and upset operating conditions, such as flow induced vibration and vortex shedding, are included in the analysis.

3. (a) Indicate the allowable stress limit in membrane plus bending for the divider plate material.

   (b) Indicate the location in the divider plate where the maximum membrane plus bending stress intensity occurs, and show that it is below the limit in part (a).

Westinghouse Electric Corporation
Power Systems Company

PWR Systems Division
Box 355
Pittsburgh Pennsylvania 15230

December 19, 1975

NS-CE-885

Mr. D. B. Vassallo, Chief
Light Water Reactors
Project Branch 1-1
Division of Reactor Licensing
Attn: Mr. Raymond R. Maccary
Assistant Director for Engineering
Division of Systems Safety
Office of Nuclear Reactor Regulation
United States Nuclear Regulatory Commission
Washington, DC 20555

Dear Mr. Vassallo:

Enclosed are fifteen (15) copies of the additional information requested in your letter of November 12, 1975 in order to complete your review of Westinghouse Electric Corporation topical report WCAP-7832 (non-proprietary) entitled "Evaluation of Steam Generator Tube, Tubesheet and Divider Plate under Combined LOCA plus SSE Conditions."

WCAP-7832, submitted in December 1973, presents a detailed analysis of the steam generator structural design to demonstrate its capability to sustain stresses resulting from simultaneous LOCA and SSE loading conditions. We trust that your review of this added information will provide the desired clarification.

Your letter referred to your review schedule for this WCAP. Westinghouse wishes to be advised of the details of that schedule. This report has provided much of the material used mutually by the Technical Review Staff and by Westinghouse in the ongoing public hearings dealing with steam generator integrity and is expected to be instrumental to the eventual resolutions reached in those hearings.

Westinghouse considers that timely completion of your review and approval of this document would prove mutually beneficial for its use in safety analysis reports. We request that you consider this desire when setting the schedule for completion.

Very truly yours,

C. Eicheldinger

C. Eicheldinger, Manager
Nuclear Safety Department

CE/lz
Enclosures

ATTACHMENT

1. Your request for information regarding the apparent increase in strength of service exposed tubes compared to virgin material* is answered as follows. The lead plug tests which were referenced had as their objectives determination of possible significant changes in ductility as a function of surface exposure. All of the service exposed tubes without cracks came from one tube, and thus one heat of Inconel. The virgin material, on the other hand, was also from one different lot of Inconel. Thus the apparent differences in flow strength represent the normal variations in yield strength exhibited by Inconel 600 tubing. For example, a review of mill records for HAPD Inconel varied in yield strength from 38,500 to 65,500. This indicates that considerable variation in yield strength is typical of normal production material.

*Inconel tubing exposed to primary cooling chemistry for one year, W Forest Hills loop setup.

2a The term stress intensity is defined as per ASME Code paragraph NB-3213.11, Section III, 1974.

2b As per Section III of the ASME Code, the Faulted Condition must consider Primary Stresses. The Primary Stresses of LOCA + SSE are the result of the rarefaction wave, the LOCA shaking, and the SSE event. WCAP-7832 and related attachments addressed these stresses. Stresses due to tube vibration at 100% load were not considered in the WCAP due to their relative minor contribution. Investigation of these tube stresses for healthy Series 51 and Model D tubes shows that the maximum bending stresses are less than 3.6 ksi at the top of the U-Bend of the outermost tube. The bending stress due to tube vibration at the top tube support plate for each is 1 ksi. The top tube support is the location of maximum stress due to the LOCA + SSE event, and the addition of this tube vibration stress would produce a negligible effect. This is shown as follows: In a thinned tube this bending due to vibration will result in a stress of 1.6 ksi for a model D tube thinned to .026 "and a stress of 2.2 ksi for a Series 51 tube thinned to .021".

The worst of all the above cases, the thinned Series 51 tube, will result in a total Stress Intensity of 77.3 ksi, this is less than the Section III Code allowable of 78.7 ksi.

3a The allowable stress limit in membrane plus bending for the divider plate material for Faulted Conditions is taken from Appendix F of Section III of the ASME Code and is 1.5(.7)(Su) = 72.4 KSI.

3b By virtue of the full constraint at the periphery of the divider plate, the bending stresses in the divider plate are secondary in nature. This categorization of stress is appropriate as it has been shown that the perimeter of the divider plate meets Section III code allowable for primary membrane stress.

ATTACHMENT

ADDITIONAL INFORMATION FOR WCAP-7832 REVIEW

This WCAP presents an analysis of the Steam Generator structural integrity, as designed, to demonstrate its capability to withstand the combined stresses of a LOCA and a SSE. Detailed discussion of various off-design situations and other accidents are not considered germane to that purpose. However, for additional clarification, responses to questions 2Ac, 2Ad, 2Ba, 2Bb, and 2Bc have been provided.

AEC Question 1: The steam generator described in RESAR-3 contains a preheater section consisting of a baffle plate and tube support plates attached to the baffle and to the steam generator shell. In Section 2.3 of WCAP-7832 this substructure is apparently not included in the seismic model of the steam generator. Discuss the effect of this structure on the response of this model.

Reply 1: The seismic mathematical model employed in WCAP-7832, and illustrated in figure 2.3-2, does not include a preheater section. Baffle plate spacing is uniform (50 inches) throughout the tube bundle. For a Model D Steam Generator, baffle spacings are considerably shorter in the preheater region. Consequently, natural frequencies of tubes in preheater regions are higher than those of the model employed in WCAP-7832. As a result, tube stresses derived from seismic inertia loads reported for the tubesheet region in WCAP-7832 are conservative.

AEC Question 2.A.a.: Provide a description of the computer program STASYS used in the tube analysis.

Reply 2.A.a.: The STASYS computer program provides a procedure for the solution of a large class of one, two, and three-dimensional structural analysis problems. Included among the capabilites of STASYS are static elastic and plastic analysis, steady state and transient heat transfer, dynamic mode shape analysis, linear and non-linear dynamic analysis, and plastic dynamic analysis.

The method of analysis used in STASYS is based on the finite element idealization of the structure. The matrix displacement method is used for each

finite element. The governing equations for each element are assembled into a system of simultaneous linear equations for the entire structure. A "wave front" direct solution technique is employed to give accurate results in a minimum of computer time.

The library of finite elements includes spars, beams, pipes, plane and axisymmetric triangles, three dimensional solids, plates, plane and axisymmetric shells, three dimensional shells, friction interface elements, springs, masses, dampers, thermal conductors, hydraulic conductors, convection elements, and radiation elements.

SUMMARIZED DESCRIPTION OF SYASYS

TYPES OF ANALYSES

In this section the various types of analyses available in the STASYS program are discussed. Included in each discussion are the basic equations being solved and any other general comments as may be applicable.

1. STATIC ANALYSIS

1.1 Static Elastic Analysis

The static elastic analysis option of the program is used to solve for the displacements and stresses in a linear elastic structure under the action of applied displacements, forces, pressures, and temperatures.

Static Elastic Analysis Theory

The basic equation for the static analysis is

$$[K]\ \{\Delta x\} = \{\Delta F_{app}\} + \{\Delta F_{pres}\} + \{\Delta F_{th}\} \qquad (2\text{-}1)$$

where

$[K]$ is the structure stiffness matrix, which is the sum of the element stiffness matrices.

$\{\Delta x\}$ is the incremental displacement vector due to the applied load increment.

$\{\Delta F_{app}\}$ is the applied nodal force increment

$\{\Delta F_{pres}\}$ is the nodal force increment due to the applied pressure load increment.

$\{\Delta F_{th}\}$ is the nodal force increment due to the applied temperature increment.

For a single load case, the incremental solution is identical to the total solution, and equation 2-1 becomes:

$$[K]\ \{x\} = \{F_{app}\} + \{F_{pres}\} + \{F_{th}\} \qquad (2\text{-}2)$$

The set of simultaneous linear equations in Equation 2-1 (or 2-2) is solved by the Wave Front Equation Solver, a direct solution technique. The maximum number of degrees of freedom on the wave front at any time during the solution is limited by core storage to about 150.

The resulting solution vector is printed out and used to calculate the stresses in the elements. If more than one load set acts on the structure, the incremental displacement solutions are summed and the element stresses are the total stresses due to all the load increments.

1.2 Static Plastic Analysis

The static plastic analysis option of the program is used to solve for the displacements, strains, and stresses in a structure or body undergoing plastic deformation. The solution is limited to problems where the deflections are small. The boundary conditions may be applied displacements, forces, pressures and/or temperatures.

The program uses the Von Mises yield criteria and the Prandtl-Reuss flow equations. The stress-strain relationship is defined by the user as a tabular function of temperature. Unloading and reversed loading is allowed, with kinematic hardening applied in the case of stress-reversal.

At each loading level an elastic solution for incremental displacements is obtained, the amount of plastic flow determined, and the load vector for the next load increment is modified to account for this plastic flow increment. This procedure causes the calculated plasticity to lag the loading increment, resulting in calculated stresses which are somewhat higher than the true stresses. The solution can be refined by taking smaller load increments or by iterating more times at each load increment. If several iterations are done at a given load step the program uses an extrapolation procedure to estimate the plastic strain at the next load step, giving a plastic solution which converges quite rapidly.

Static Plastic Analysis Theory

The basic equation for the static plastic analysis is:

$$[K]\ \{\Delta x\} = \{\Delta F_{app}\} + \{\Delta F_{pres}\} + \{\Delta F_{th}\} + \{\Delta F_{plast}\} \qquad (2\text{-}3)$$

$\{\Delta F_{plast}\}$ is the nodal force increment due to the plasticity which occurred during the previous load step (or estimated for this load step)

The resulting simultaneous linear equations are solved by the Wave Front Equation Solver, as in the elastic analysis.

2. THERMAL AND FLOW ANALYSES

2.1 Steady State Thermal Analysis

The steady state thermal analysis option is used to solve for the steady state temperature distribution in a heat conducting body. The boundary conditions may be specified temperatures or specified heat flow rates. Convection and radiation elements are included so that convection and radiation boundary conditions can be handled. The material properties may be temperature dependent, which, along with the radiation element, causes a non-linear problem and requires an iterative solution.

Steady State Thermal Analysis Theory

The basic equation for the steady state thermal analysis is

$$[K_T]\ \{T\} = \{Q_{app}\} + \{Q_{gen}\} \tag{2-4}$$

where

$[K_T]$ is the structure thermal conductivity matrix, which is the sum of the element conductivity matrices.

$\{T\}$ is the nodal temperature vector, which is the solution of the set of simultaneous equations.

$\{Q_{app}\}$ is the applied heat flow rate at the nodes (if any).

$\{Q_{gen}\}$ is the heat flow at the nodes due to internal heat generation in the elements.

The set of linear equations in Equation 2-4 is solved by the Wave Front Equation Solver. The resulting solution vector of nodal displacements is printed out. If the thermal conductivity of the material is temperature dependent or if there are radiation elements the calculated temperature distribution is used for the calculation of the conductivity matrix for the next iteration.

2.2 Transient Thermal Analysis

The transient thermal analysis option of the program is used to solve for the nodal point and element temperatures as a function of time.

The effect of temperature dependent material properties and radiation boundary conditions is included by evaluating the material properties and radiation heat transfer coefficient based on the most recently calculated temperature.

2.2.1 Transient Thermal Analysis Theory

The basic equation for the transient thermal analysis is:

$$\frac{1}{\Delta T}[C_T] + [K_T] \quad T_n = Q_{app_n} + Q_{gen_n} + \frac{1}{\Delta T}[C_T] \quad T_{n-1} \qquad (2\text{-}5)$$

where

ΔT is the time difference between the time at step n and the time at step n-1

$[C_T]$ is the specific heat matrix for the entire model

$[K_T]$ is the thermal conductivity matrix for the entire model

T_n is the (unknown) vector of nodal temperatures at time n

Q_{app_n} is the applied nodal heat fluxes at time n

Q_{gen_n} is the nodal heat fluxes due to the internal heat generation at time n

T_{n-1} is the (known) vector of nodal temperatures at time n-1

The resulting simultaneous linear equations are solved by the Wave Front Equation Solver at each time point during the transient.

2.2.2 Steady State Hydraulic Analysis

The steady state hydraulic analysis option of the program can be used to solve the flow balance problem in the network of flow paths (pipes). The program calculates the pressure at each node of the model and the flow rate in each fluid passage.

The flow balance problem is non-linear, and requires an iterative solution. The boundary conditions are applied as a step and a number of iterations are done to determine the solution. Additional sets of boundary conditions can be applied for other solutions.

The solution technique used seems to be rapidly convergent, and about 5 iterations usually gives a reasonable convergence.

Steady State Hydraulic Analysis Theory

The basic equation for the steady state hydraulic analysis is:

$$[K_H]\ \{\sqrt{p}\ \} = \{\dot{W}_{app}\} \tag{2-6}$$

where

$[K_H]$ is the hydraulic conductance matrix for the entire flow network.

$\{\sqrt{p}\ \}$ is the vector of the square roots of the nodal point pressure

$\{\ \dot{W}_{app}\ \}$ is the flow rates applied to the nodal points

The resulting set of equations is non-linear in pressure because of the square root term, so an iterative solution procedure is used.

3. MODAL ANALYSES

There are two options available for modal analyses. The first option considers all the degrees of freedom in the structure and does not require specification of dynamic degrees of freedom. It can be used for small problems with less than 85 degrees of freedom. The second option requires the specification of dynamic degrees of freedom and can handle much larger structures.

3.1 Standard Modal Analysis

The standard modal analysis is used to determine the natural frequencies and mode shapes for a linear elastic undamped structure. This analysis calculates the complete set of eigenvalues and eigenvectors for the model, and is limited to models having less than 85 unrestrained degrees of freedom.

The structure must be a linear elastic structure. If damping is present in the model it is ignored, if non-linear elements are present they are treated as linear, with their stiffness depending on their initial state (a gap will produce no stiffness, a closed interface will have the interface stiffness).

<u>Standard Modal Analysis Theory</u>

The basic equation for the dynamic behavior of a structure is:

$$[M]\{x\} + [C]\{\dot{x}\} + [K]\{x\} = \{F(t)\}$$

where

- [M] is the total mass matrix of the structure, the sum of the individual element masses,
- [C] is the total viscous damping matrix of the structure, the sum of the individual element damping matrices,
- [K] is the total stiffness matrix of the structure, the sum of the individual element stiffness matrices,

$\{x\}$ is the nodal point displacement vector,

$\{\dot{x}\}$ is the nodal point velocity vector,

$\{\ddot{x}\}$ is the nodal point acceleration vector, and

$\{F(t)\}$ is the vector of applied nodal forces as functions of time, t.

In the case of an undamped structure under free vibrations Equation 2-7 becomes

$$[M]\{\ddot{x}\} + [K]\{x\} = 0 \tag{2-8}$$

If it is assumed that the motion is harmonic of the form

$$\{x\} = \{x_o\} \cos\omega t \tag{2-9}$$

Equation 2-8 becomes

$$[K]\{x_o\} = \omega^2 [M]\{x_o\} \tag{2-10}$$

which is an eigenvalue problem, and is often written

$$[K][\Psi] = [\lambda][M][\Psi] \tag{2-11}$$

where

$[\Psi]$ is the modal matrix,

$[\lambda]$ is the diagonal matrix whose terms are the squares of the natural frequencies.

The equation in 2-11 is transformed to the classical eigenvalue problem

$$[K][\Psi] = [\lambda][\Psi] \tag{2-12}$$

and then solved by a Jacobi reduction.

The Jacobi reduction has the advantages of speed and accuracy, yielding a complete set of eigenvalues and eigenvectors.

3.2 Reduced Modal Analysis

The reduced modal analysis option is used to determine the natural frequencies and mode shapes for a linear elastic, undamped structure. This analysis requires the specification of dunamic degrees of freedom of the model, which are a subset of the total number of degrees of freedom. The dynamic degrees of freedom are chosen so as to characterize the deformations of the structure in the various modes of interest. The total number of degrees of freedom in the model can be as large as for static problems, but the number of dynamic degrees of freedom must be less than 85. 85 modes are usually ample for a modal analysis of any reasonable structure.

The structure must be a linear elastic structure. If damping is present in the model it is ignored, and any non-linear elements present are treated as linear, with their stiffness depending on their initial state (a gap will produce no stiffness, a closed interface will have the interface stiffness).

3.2.1 Reduced Modal Analysis Theory

The basic equations for the reduced modal analysis are the same as those for the standard modal analysis (Equations 2-7 through 2-12) except that the mass and stiffness matrices are reduced to contain only the specified dynamic degrees of freedom.

The reduced stiffness matrix can be thought of as the matrix of the influence coefficients of the structure at the points and in the directions of the dynamic degrees of freedom, while the reduced mass matrix results from a redistribution of the mass to the dynamic degrees of freedom in a manner consistent with the possible static deformations of the structure due to imposed deformations along the dynamic degrees of freedom.

4. HARMONIC RESPONSE ANALYSES

4.1 Harmonic Response Analysis

The harmonic response analysis is a steady state solution of a linear elastic system under a set of harmonic loads of known amplitude and frequency. These boundary loads may be specified displacements, forces, or pressures. All forcing functions for a given analysis must be at the same frequency and in phase. Damping is allowed in the system, either as discrete viscous dampers or as a damping matrix which is a specified linear combination of the mass and stiffness matrices.

4.1.1 Harmonic Response Analysis Theory

As in the modal analysis, the basic equation for the dynamic behavior of a structure is:

$$[M]\{\ddot{x}\} + [C]\{\dot{x}\} + [K]\{x\} = \{F(t)\} \qquad (2\text{-}13)$$

where the terms are defined following Equation 2-7.

Assuming the forcing function is of the form

$$\{F(t)\} = \{F_o\}\, e^{j\omega t} \qquad (2\text{-}14)$$

and the displacement is of the form

$$\{x\} = \{x_o\}\, e^{j\omega t} \qquad (2\text{-}15)$$

then Equation 2-13 becomes

$$-\omega^2 [M] + j\omega [c] + [K] \quad \{x_o\} = \{F_o\} \qquad (2\text{-}16)$$

This is a set of simultaneous linear equations of the same form as for the static elastic solution, except that the matrix is complex.

The solution will have a displacement vector x_o which is complex, having a real and an imaginary portion, representing an amplitude and a phase angle. If there is no damping in the system the imaginary portion will be 0.0, representing a zero phase angle and the response is in phase with the forcing function.

5. NON-LINEAR DYNAMIC TRANSIENT ANALYSES

5.1 Non-linear Dynamic Transient Analysis

The non-linear dynamic transient analysis is a time-history solution of the response of an arbitrary structure to a known force and/or displacement forcing function. The structure may include non-linear elements, gaps, interfaces, plastic elements, and viscous and Coulomb dampers. Allowed forcing functions include nodal displacements, nodal forces, pressures, and/or temperatures. Output includes displacements and stresses as a function of time for the complete structure.

Non-Linear Dynamic Transient Analysis Theory

As in the modal analysis and the harmonic response analysis, the basic equation for the dynamic behavior of a structure is:

$$[M]\{\ddot{x}\} + [C]\{\dot{x}\} + [K]\{x\} = \{F(t)\} \qquad (2\text{-}17)$$

where $\{F(t)\}$ may include the effects of applied displacements, forces, pressure, temperatures, or non-linear effects such as plasticity.

If $\{x_t\}$ is assumed to be either of the form

$$\{x_t\} = \{a\} + \{b\}t + \{c\}t^2 \qquad \text{(quadratic)} \qquad (2\text{-}19)$$

or

$$x_t = \{a\} + \{b\}t + \{c\}t^2 + \{d\}t^3 \qquad \text{(cubic)} \qquad (2\text{-}19)$$

then

$$\{\dot{x}_t\} = \{b\} + 2\{c\}t \qquad \text{(quadratic)} \qquad (2\text{-}20)$$

$$\{\dot{x}_t\} = \{b\} + 2\{c\}t + 3\{d\}t^2 \qquad \text{(cubic)} \qquad (2\text{-}21)$$

and

$$\{\ddot{x}_t\} = 2\ \{c\} \qquad \text{(quadratic)} \qquad (2\text{-}22)$$

$$\{\ddot{x}_t\} = 2\ \{c\} + 6\{d\}t \qquad \text{(cubic)} \qquad (2\text{-}23)$$

Equation 2-18 and 2-19 can also be solved for {a}, {b}. {c}, and {d} in terms of the displacement at times t, t-1, t-2, etc., to give:

$$\{\dot{x}_t\} = f_1\ (\{x_t\},\ \{x_{t-1}\},\ \{x_{t-2}\},\ .\ .\ .\ ) \qquad (2\text{-}24)$$

$$\{\ddot{x}_t\} = f_2\ (\{x_t\},\ \{x_{t-1}\},\ \{x_{t-2}\},\ .\ .\ .\ ) \qquad (2\text{-}25)$$

Substituting the expressions (2-24) - (2-25) into Equation 2-17 gives

$$\frac{C_1}{\Delta T^2}\ [M] + \frac{C_2}{\Delta T}\ [C] + [K] \quad \{x_t\} = \{F_{(t)}\} + f \quad [M],\ [C],$$

$$\{x_{t-1}\},\ \{x_{t-2}\},\ .\ .\ .\ . \qquad (2\text{-}26)$$

This equation can be solved for x_t in terms of the previous (known) values of the nodal displacements. Since [M], [C], and [K] are included in the equation, they can also be time or displacement dependent.

6. LINEAR DYNAMIC TRANSIENT ANALYSES

6.1 Linear Dynamic Transient Analysis

The linear dynamic transient analysis is a time-history solution for the response of a linear elastic structure to a known force and/or displacement forcing function. The structure must not contain any non-linear elements or include any damping. No element loads (pressure or temperature) are allowed. The solution proceeds in two stages - a complete pass through the transient to determine the displacement history, followed by a second pass (if desired) to calculate the element stresses over a usually coarser time interval.

Linear Dynamic Transient Analysis Theory

The equations used in the linear dynamic transient analysis are similar to those in the non-linear analysis except for two modifications.

The linear structure has constant [M] and [K] matrices, so the equation 2-7 can be reduced to a smaller number of dynamic degrees of freedom as is done in the reduced modal analysis.

Equation 2-26, when written in terms of the reduced matrices and restricted to a constant Δt can be inverted to obtain:

$$\{x_t\} = [\overline{K}]^{-1} \quad \{F(t)\} + f([M], \{x_{t-1}\}, \{x_{t-2}\}, \text{etc.}) \qquad (2\text{-}27)$$

where

$$[\bar{K}]^{-1} = \frac{C_1}{\Delta t^2} [M] + [K]^{-1} \tag{2-28}$$

This reduces the solution for the dynamic degrees of freedom to a series of relatively small matrix multiplications after having once found the $[\bar{K}]^{-1}$ matrix.

Once the displacements at the dynamic degrees of freedom are known as a function of time the stress solution at any time in the transient can be calculated.

AEC Question 2.A.b.: Provide the basis for the assumed 40 year thinning.

Reply 2.A.b.: The 40 year thinning allowance (0.003 in.) is intended to account for the corrosive effects of Reactor Coolant Fluid flowing within Inconel Steam Generator tubing. A conservative weight loss rate of 11.5 mg./ dm^2 - mo. (31.9 mg./dm^2 in 2000 hrs.) is obtained from reference 1 for Inconel in flowing 650°F primary fluid. For comparative purposes, a weight loss rate of 15.4 mg/dm^2 in 2000 hrs (5.55 mg/dm^2-mo.) for stabilized Inconel, obtained in reference 2, is often referred to, as a worst case rate. The equivalent thinning rate* is 0.017 mils/year. This rate is, essentially, short term data which, if projected over 40 years, would result in 0.680 mils thinning. Reference 3 (page 137) indicates that the corrosion rate is reduced by approximately a factor of 10, after 5000 hours. The total expected corrosive thinning in 40 years on the inner tubing surface is found by combining the initial rate for the first year (8760 hrs) with a rate reduced by 9/10 for 39 years: $(0.017 \frac{\text{mils}}{\text{yr}} (1 \text{ yr}) + (0.017 \frac{\text{mils}}{\text{yr}}) (\frac{1}{10}) (39 \text{ years}) = 0.083$ mils. The assumed 3 mil thinning rate in WCAP-7832, therefore, allows 2.917 mils for general, uniform corrosive thinning on the secondary side. This allowance is conservative in comparison with Ref. 2 test data on Inconel in simulated secondary water chemistry which indicates that the weight loss rate is of the same order of magnitude as for primary water chemistry. The 3 mil allowance assumed in WCAP-7832 is for uniform corrosion only.

The local corrosive attack on the secondary surface which has been observed recently on some plants is not included in the thinning allowance. The local attack is associated with sludge deposits and local chemical-hydraulic interactions. Control and prevention of this local effect are contemplated by proper secondary water chemistry.

References (Reply 2.A.b.)

1. Berry, W. E., Stiegelmeyer, W. N., Fink, W. F., "The Corrosion of Inconel in High-Temperature Water (Phase II), "Battelle Memorial Institute, December 15, 1958.

*- Equivalent to 11.5 mg/dm^2 - mo.

2. Berry, W. E. and Fink, W. F., "The Corrosion of Inconel in High-Temperature Water, "Battel Memorial Institute, April 4, 1958.

3. Depaul, D. J., "Corrosion and Wear Handbook for Water Cooled Reactors," USAEC, TID 7006, March 1957.

AEC Question 2.A.c.: Provide a reference or additional data on crack propagation tests on tubes loaded by combined internal pressure and axial bending moments.

Reply 2.A.c: External bending loads have an influence on the burst pressure of flawed tubes. This effect has been observed at bending stress levels up to 34,000 psi and is considered insignificant in that range (0-34,000 psi). Tube movements, induced for example by a seismic event, can generate bending stress which may facilitate plastic bulging of the crack area. However, while bending stresses lower the pressure at which point stresses exceed the yield strength, it is not certain that such stresses greatly affect the fully plastic limit pressure of flawed tubes.

Examination and testing of tube specimens removed from operating steam generators which have surface stress-corrosion cracks have indicated that the ductibility of the uncracked tube material has not degraded. Several tests were conducted with bending stresses superimposed on internally pressurized tubes to determine if this load would accelerate crack propagation. It is concluded from those tests that there is no strong effect of bending stress on crack propagation. Further discussion, data, and SEM photographs are included in the response to question 2Bd, and the test data of Table III-3.

Table III-3 lists the burst pressure of tubes with through wall slits subjected to combined bending and internal pressure. At an outer fiber stress of 34,000 psi the largest effect on the burst pressure is less than a ten percent decrease. The bending load was applied (on different samples) with the crack located on the neutral axis, and on both the tension and compression sides of the tube (beam).

Higher bending stresses could not be investigated due to a tube collapse limiting condition at the points of load application. A significant affect on burst pressure is possible at higher bending stress levels but none was observed at 34,000 psi. For comparison, note that the bending stress calculated on pg. 3.1-15 is 23,000 psi. For comparison, note that the bending stress calculated on pg. 3.1-15 is 23,000 psi for a tube wall thinned to 0.026 in. Most likely bending stress will only have a strong effect on the burst strength of flawed tubes at a bending moment close to the limit moment of the tube.

TABLE III-3

COMBINED BENDING AND INTERNAL PRESSURE BURST TESTS

Specimen Number	Burst Pressure (psi)	Load, P (lbs)	Maximum Outer Fiber Stress (psi)	Flaw Location
3742-.8-BB-T	2800	1875	34,000	Tension Side (1)
3742-.8-BB-C	2350	1875	34,000	Compression Side (2)
3742-.8-BB-N	2400	1875	34,000	Neutral Axis (3)
3742-.8-X	2500	0	0	---

Tube Diameter	0.875
Wall Thickness	0.050
Flaw Length	0.80 inch through wall
Temperature 75°F	

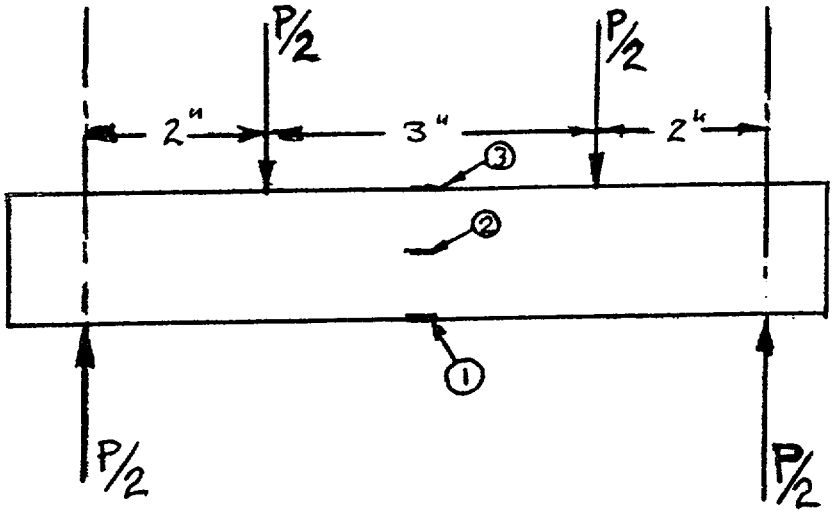

AEC Question 2.A.d.: Provide a reference or additional data on the tube collapse tests, and the analytical correlation and analysis on which the extrapolation of test results to tubes of different yield strength and wall thickness is based.

Reply 2.A.d.: Collapse tests have been conducted at the University of South Florida, Tampa, Florida, under the auspices of W Tampa Division on slightly oval (0-10%) straight and U-bend Inconel tubular specimens of various sizes. Some of the significant test results are summarized below:

Nominal Tube Size (in)			Ovality (%)				
Dia.	Thick.		0	3	5	7	10
5/8	.039	Minimum Collapse Pressure (psi)	6300	4300	4000	3750	3050
7/8	.050		6800	4500	4200	3800	3100
3/4	.043		7300	4800	4250	3850	3300

The results shown above are for straight tubular specimens. Test results indicate that collapse pressures of U-bends are higher than for straight sections as shown in attached Figure 6 of reference 1. Pressure versus ovality for straight tubes and for U-bend tubes (Inconel 600) illustrate the effect of ovality on the normalized, dimensionless collapse pressure term $\frac{p\rho}{\sigma y\ t}$ in Figure 5 of ref. 1. where: p is the pressure difference across the tube wall, ρ is the mean tube radius, σy is the yield stress, and t is the tube wall thickness.

Reference 1 (Reply 2A.d.): A. Lohmeier, and N. C. Small, "Collapse of Ductile Heat Exchanger Tubes with Ovality Under External Pressure." Presented at the 2nd International Conference on Structural Mechanics in Reactor Technology."

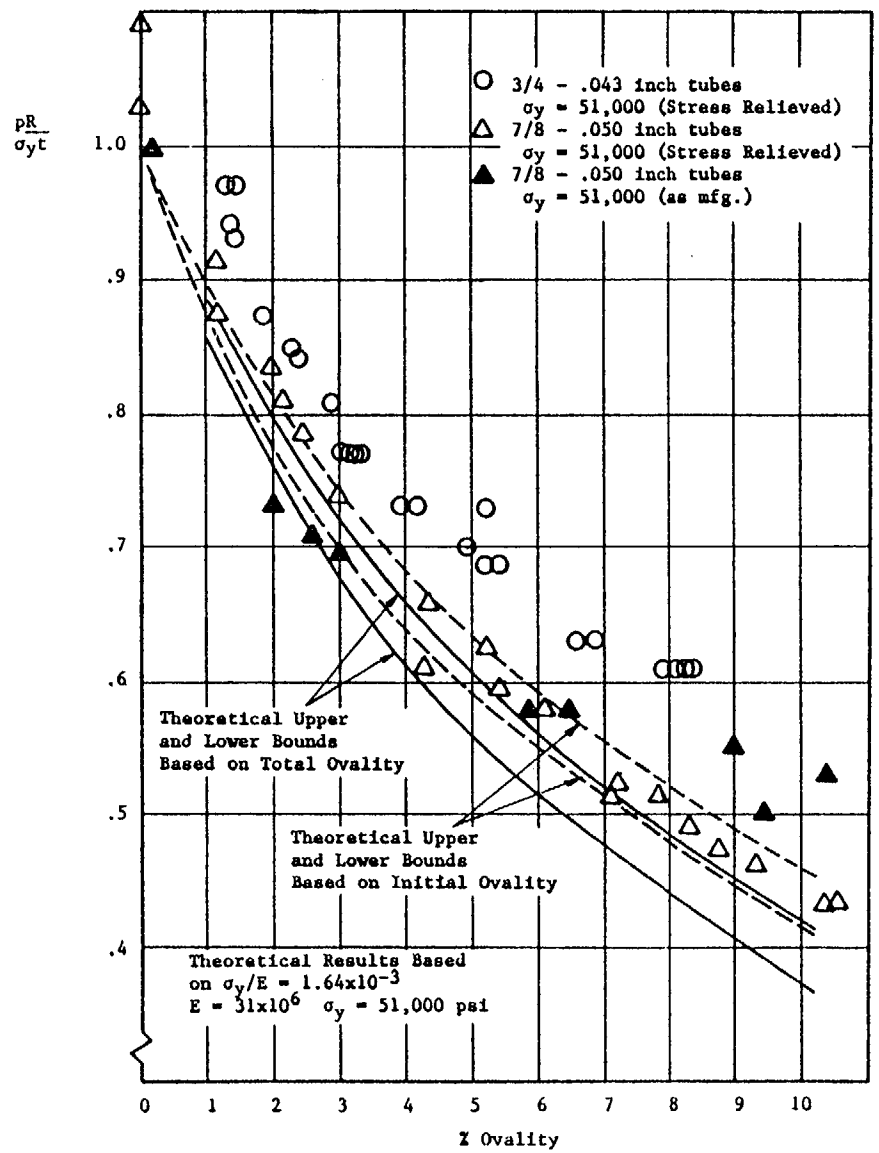

Figure 5 Comparison of Experimental Results for Collapse of Long-Oval Tubes under External Pressure with Theoretical Upper and Lower Bounds

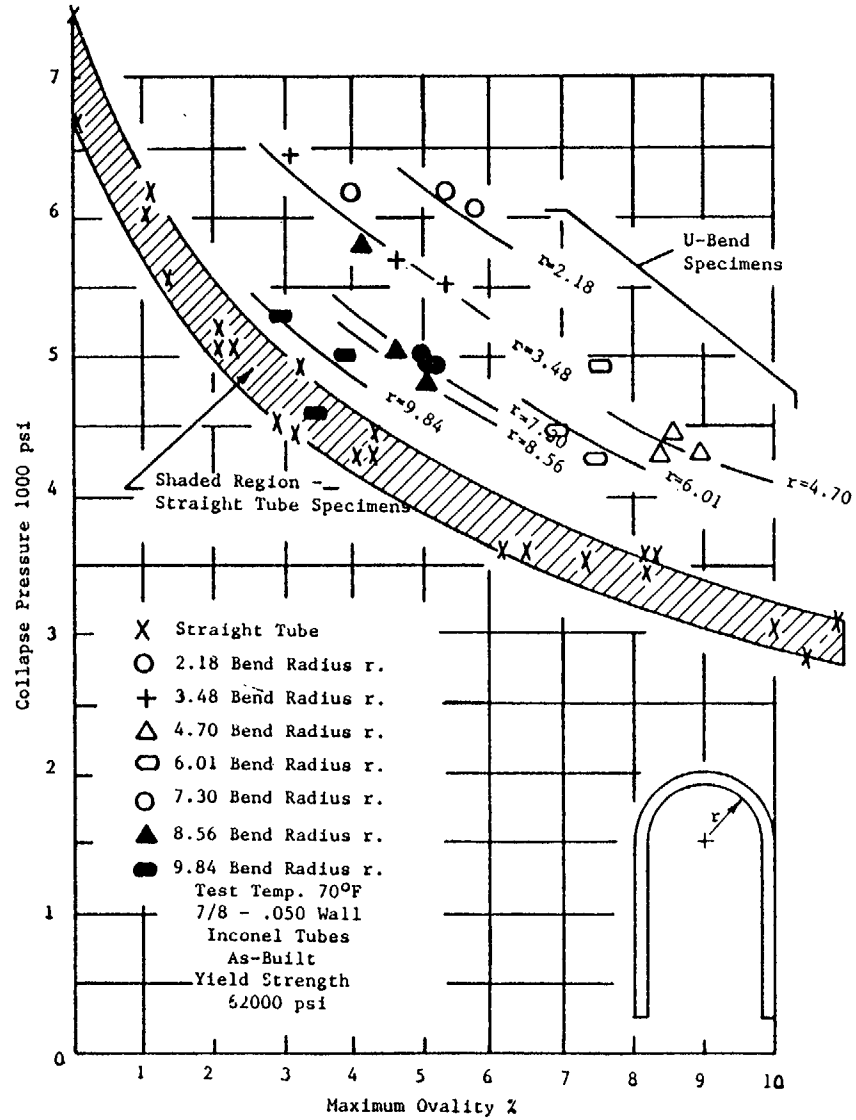

Figure 6 Experimental Results Showing Effect of Tube Bending Configuration on External Collapse Pressure

AEC Question 2.B.a.: Describe the analysis employed to assess the effect of a postulated steam line break on the steam generator tubes and provide a summary of the results.

Reply 2.B.a.: Although steam line break is not in the scope of WCAP-7832, since it evaluates LOCA plus SSE conditions, the following summary is provided: An analysis of flow induced vibration of the tube bundle following a postulated steam line break was performed. The tubes in the U-bend region were assumed to be subjected to cross-flow. Mass flow rates, fluid densities and cross-flow velocities were evaluated by a hydrodynamic analysis. Tube deformations and bending stresses were evaluated based on flow-induced vibration criteria. The flow induced vibration analysis considered both vortex shedding and fluid-elastic vibration mechanisms.

The resulting maximum tube deformation in the U-bend region is 6 mils and the corresponding maximum bending stress in the tube is 560 psi. It was concluded that these values are sufficiently small to insure the structural integrity of the Model D (preheat) tube bundle and are representative of the Model 51 series (non-preheat) Steam Generators.

AEC Question 2.B.b.: Describe the analyses employed to assess the effect of a postulated break at the feedwater nozzle on the preheater substructure and provide a summary of the results.

Reply 2.B.b.: A feedwater line break at the nozzle is not in the scope of WCAP-7832, however the following summary is provided: A structural evaluation of the Model D Steam Generator preheater region was performed for a postulated break at the feedwater nozzle. Transient pressure loadings on the preheater structure were evaluated by static three dimensional nonlinear finite element ~~analyses using amplification~~ factors to account for dynamic effects.

Maximum stresses in the components of the preheater structure were compared to allowable stress limits defined in the Subsection NG, ASME Code, Section III, for Faulted Conditions. The results are summarized below:

Location	Maximum Value	Allowable Value
Baffle Plate	P_m = 29.0 ksi	36.4 ksi
	$P_m = P_b$ = 47.8	54.6
Partition Plate	P_m = 10.0	31.1
	$P_m + P_b$ = 26.0	46.6
Impingement Plate	p = 250 psi	1110 psi

Model 51 Steam Generators which do not have a preheater section (feedwater is introduced above the tube bundle) and would behave, in a general way, similarly to a preheat generator during a steam line break.

AEC Question 2.B.c: Discuss the effects of local thinning due to wear and local crud accumulation at the tube supports on the burst strength of the tubes.

Reply 2.B.c.: A test program of tubes with simulated wear or local thinning has been run on both 7/8 in. OD and 3/4 in. OD Inconel tubing. The tubes had flats milled on the outer surface of varying axial lengths. The results, presented in Figures 4-1 and 4-2, illustrate the influence of the axial length of the thinned area on burst pressure. It can be seen that for a part wall (24-27% remaining Figure 4.1 and 19-28% on Figure 4-2 for 3/4" tubes) infinitely long defect, the burst pressure is approximately 2500 psi which is greater than plant operating pressure (with zero on the steam side). For smaller length defects, the burst pressure is substantially higher. E.g., for a 1" long, part wall defect, the burst pressure is approximately 4200 psig, and for a 1/2" long defect, the pressure is roughly 6200 psig.

Question 2.B.d.: Identify the method by which corrosion phenomena were considered in assessing the fatigue strength of the tubes.

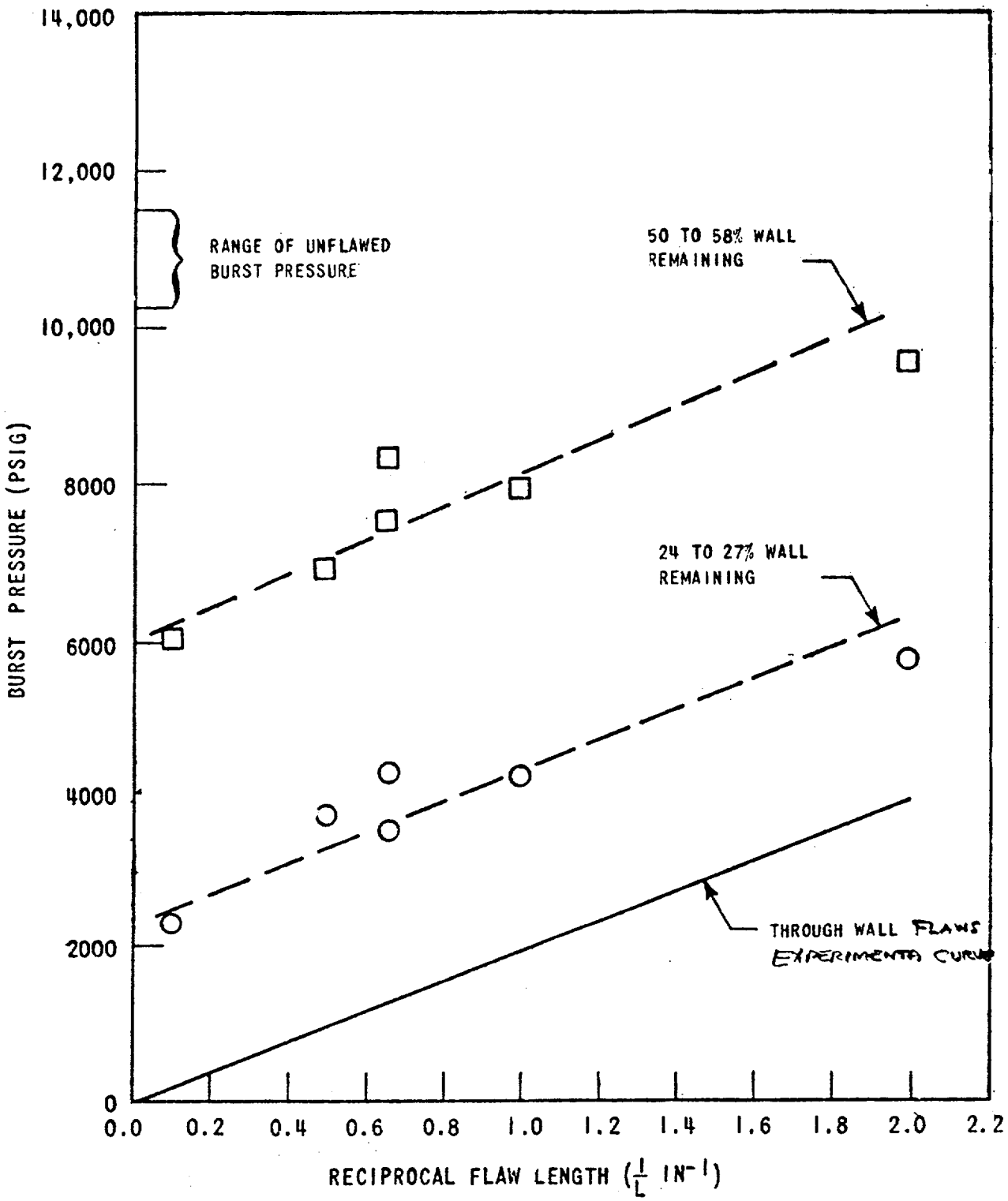

Figure 4-1 Room Temperature Burst Pressure of 7/8" Tubes with Machined Flats

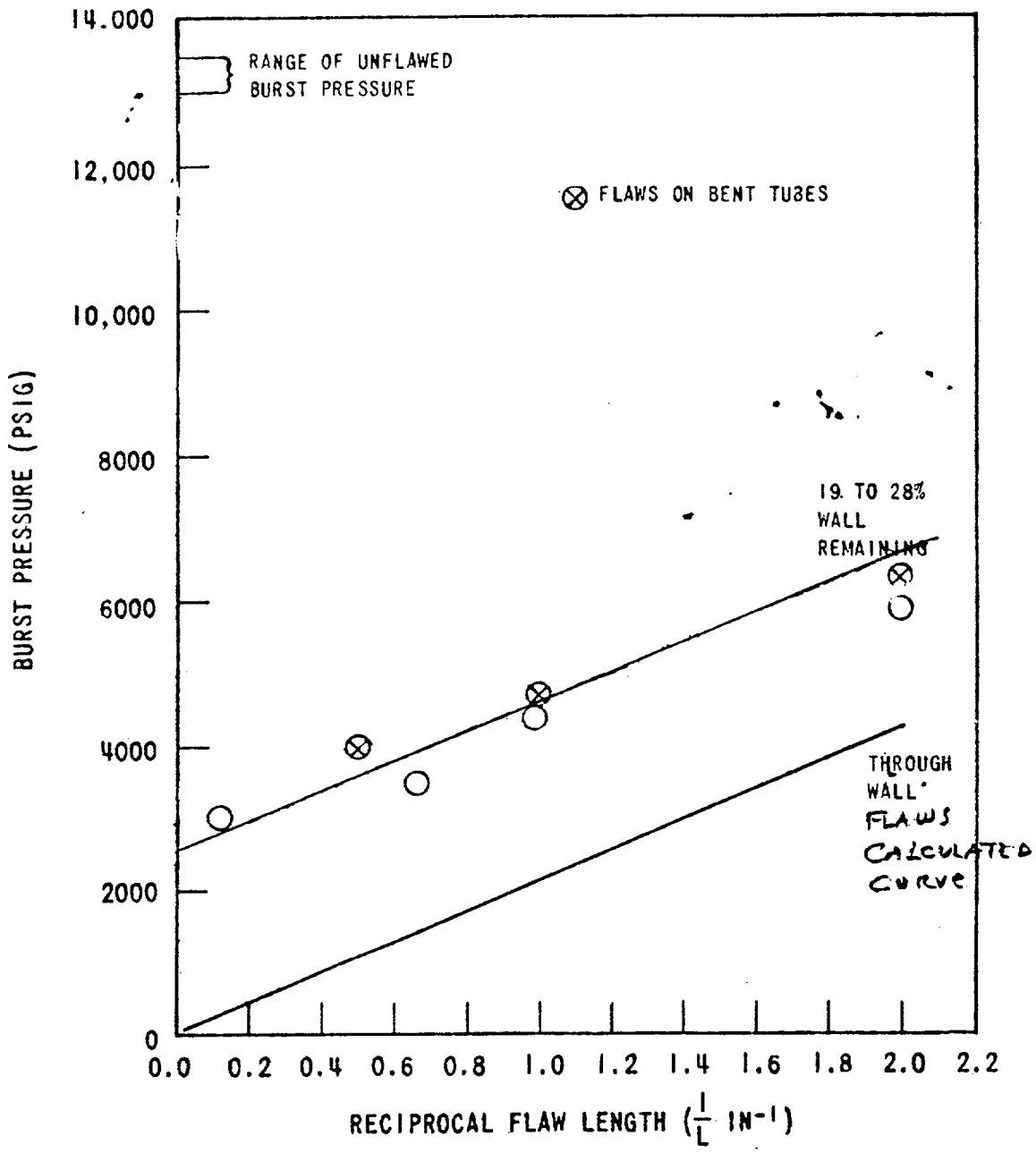

*CALCULATED

Figure 4-2 Room Temperature Burst Pressure of 3/4" Tubes with Machined Flats

Reply 2.B.d.: WCAP 7832 deals with combined LOCA plus SSE loading conditions. Since these conditions are classified as Faulted (one occurrence), a fatigue analysis is not required by the ASME Boiler and Pressure-Vessel Code, Section III.

In order to gain information on the mechanical properties and possible changes to the microstructure of tubes which have sustained port wall integranular stress corrosion cracking, burst tests and metallurigical examinations have been performed on tubes which have seen service in an operating steam generator.

For comparison, the same tests were run on virgin tubes. The test results for virgin tubes were quite reproducible. The results for the tubes with service exhibited some variations which are attributed to variations in the extent of intergranular cracking on the OD surface. Test results are shown in Figure VII-5 attached. Internal pressure was applied through a lead plug (Figure VII-1). Failure of the tubes in Figure VII-5 was by a ductile shear mode, the same as with the virgin tubes. There was no evidence of intergranular cracking in the Scanning Electron Microscope examination of Figure VII-6. A ductile failure is shown in Figure VII-7.

It is concluded that the lead plug burst tests provided a qualitative measure of the mechanical integrity of service exposed tubes. The tests revealed the presence or absence of intergranular corrosion cracks by the shape of the load-deflection curve. Uncracked, service exposed material was as strong and as ductile as virgin material, and, like virgin material, exhibited a ductile transgranular shear mode of failure.

AEC Question 3.a.: Provide a justification for using different pressure time histories in the tubesheet analysis and the divider plate analysis.

Reply 3.a.: The analysis of the tubesheet employed a pressure time history derived from a "rigid wall" hydrodynamic model of the primary loop. Since the tubesheet analysis was doen by static methods, the maximum pressure differenc across the tubesheet was multiplied by two to account for dynamic effects.

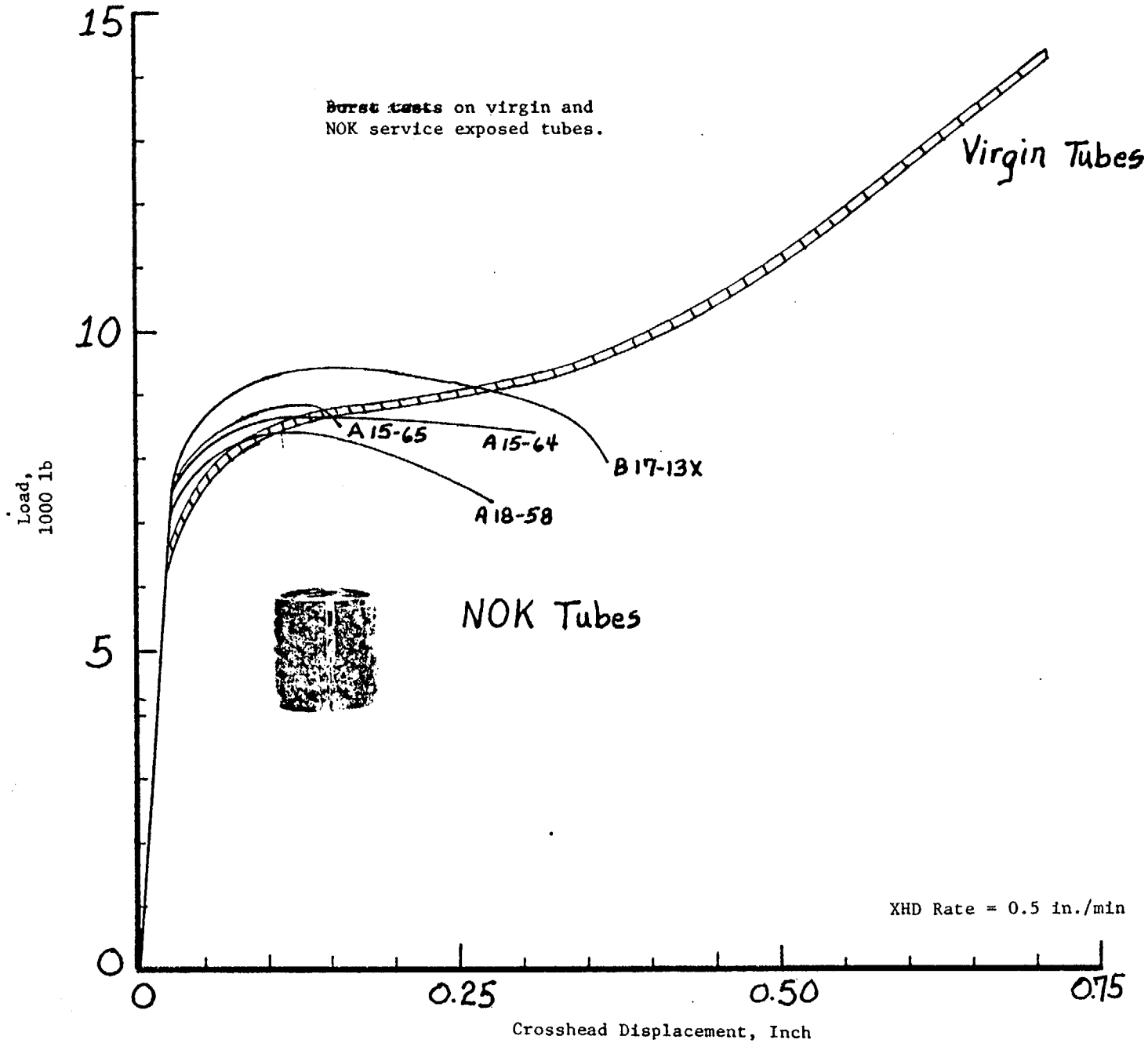

Figure VII-2

24a

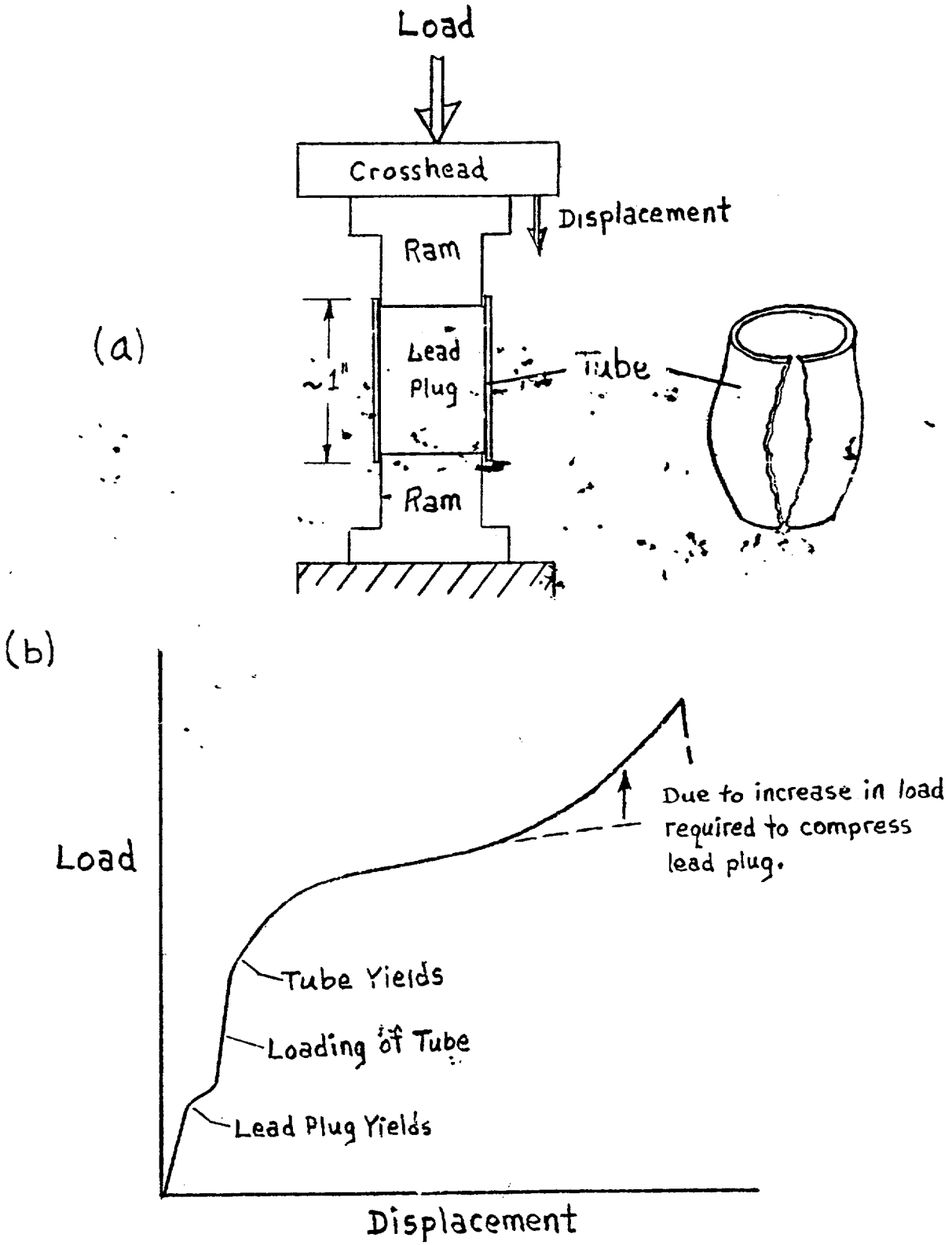

Fig. VII-1. Schematic of lead-plug burst test.

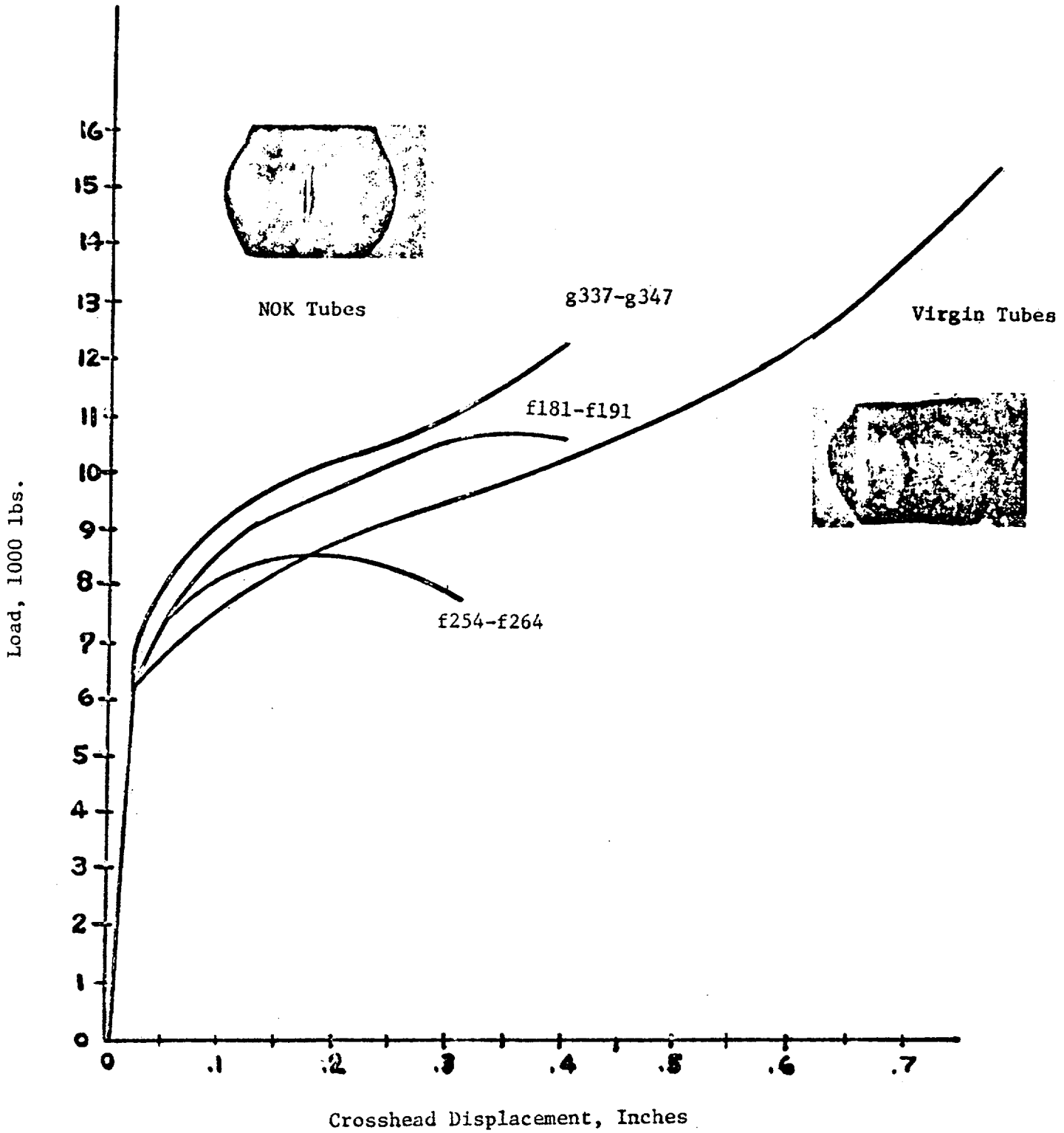

Fig. VII-4. Additional lead-plug burst test results on NOK tubes.

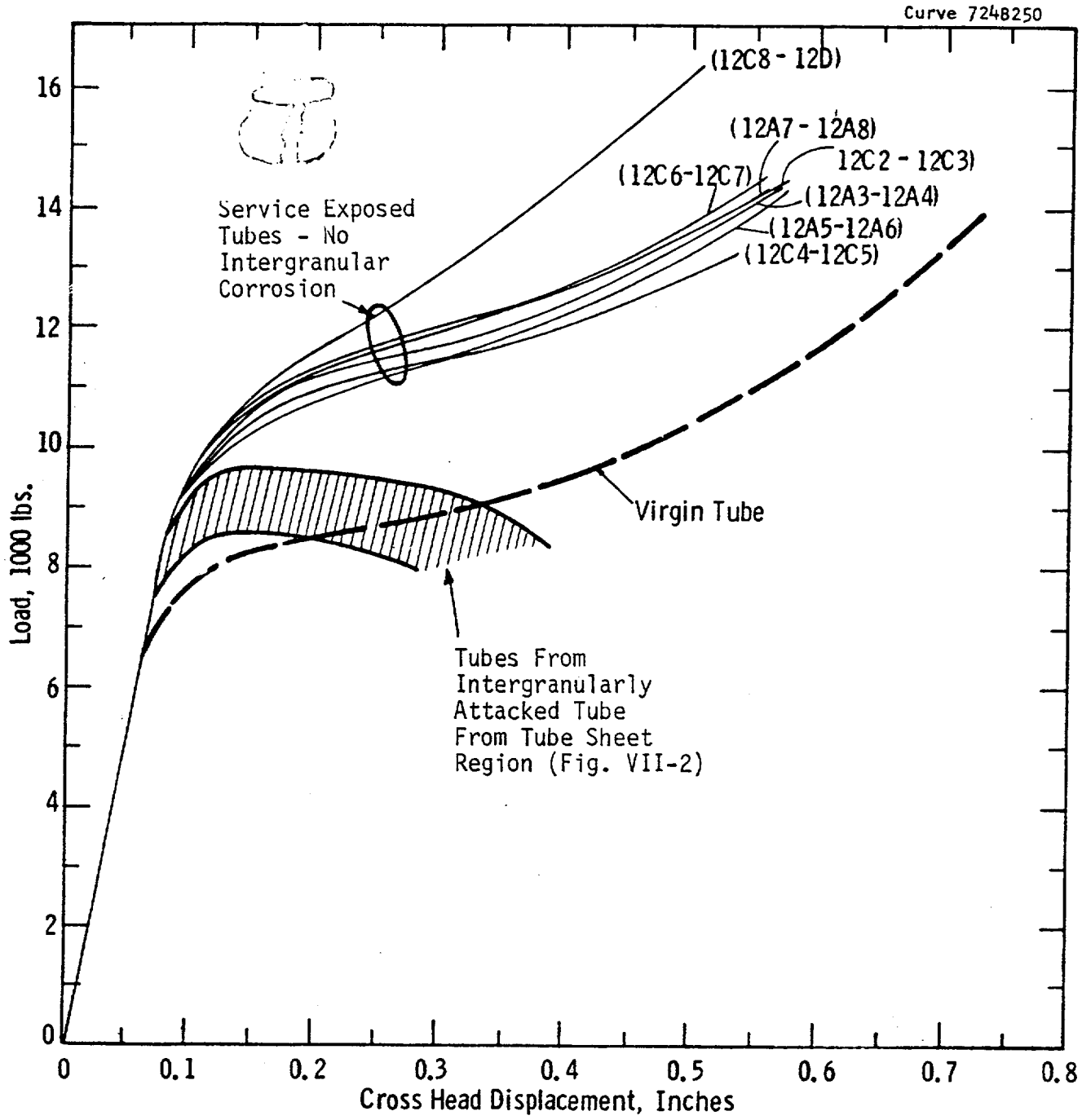

Fig. VII-5 - Lead-plug burst test results showing high ductility in virgin tubes and in tube NBK B (15-46) and reduced ductility in NOK tubes from intergranular attack in tube sheet region.

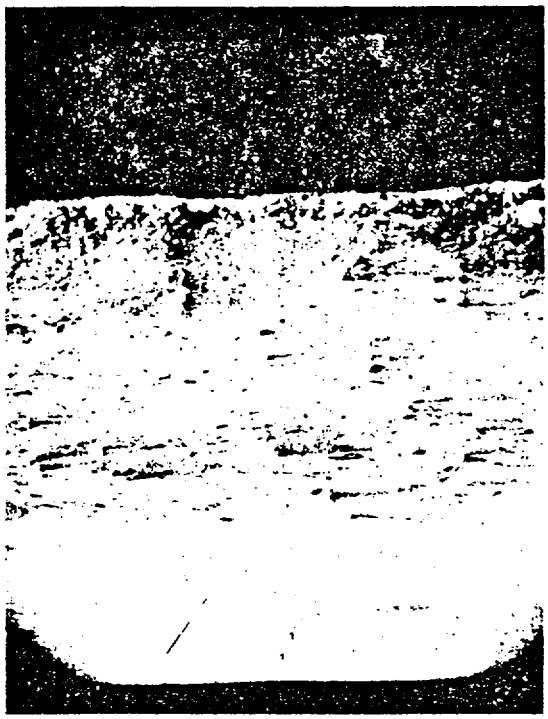

15-65
5C2

60X

15-65
5C2

I.D.

600X

15-65
5C2

O.D

600X

Figure VII-6 SEM of Fracture Surface of Tube Rupture Tests (Lead-Plug Tests) Showing Intergranular Fracture Near O.D. and Ductile Shear Area Near I.D. Tube A15-65

RM-52399

1X

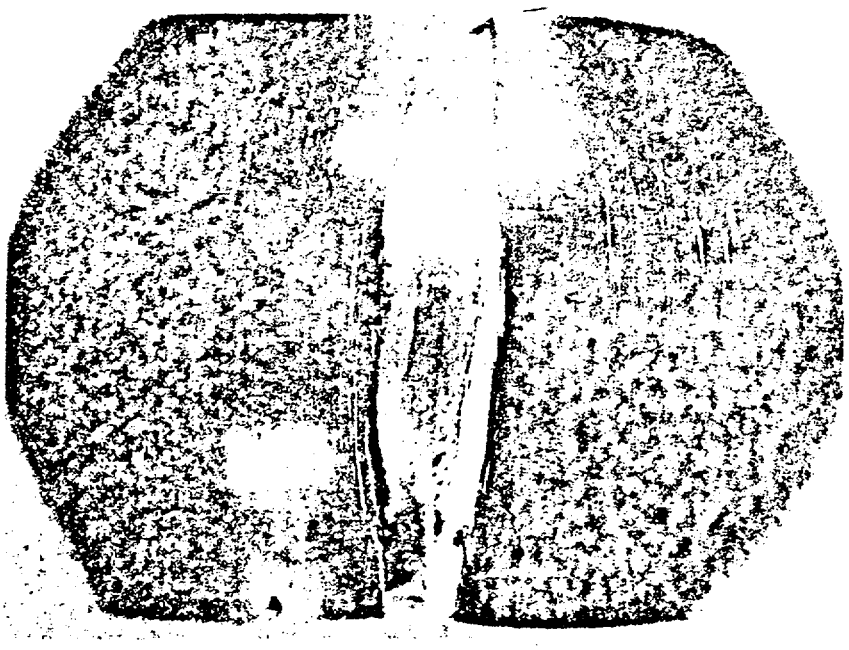

4X

Fig. VII-7 - High ductility was demonstrated after lead-plug burst test, Sec. (12A3-12A4).

FIG. VII-7

In the analysis of the divider plate, a modified pressure history based on a "flexible wall" hydrodynamic model was employed. It is well known that hydraulic transient analyses, performed with the rigid boundaries assumption, give greatly exagerated levels of the pressure fluctuations, hence, hydraulic loads, acting over the flexible boundaries. This new pressure history resulted in not only lower pressure differences across the divider plate, but also lower differences across the tubesheet. The dynamic time history analysis of the divider plate was performed using this revised pressure time history. However, since the initial conservative pressure differences across the tubesheet resulted in stress levels well below the allowable limits, it was not reanalyzed using the less conservative "flexible wall" pressure time history.

AEC Question 3.b.: Provide a comparison of the maximum deflection and stresses in the divider plate as calculated from ANSYS and PETROS.

Reply 3.b.: The analysis of the divider plate requires the evaluation of large deformations and large elastic-plastic dynamically-induced strains. The PETROS code addresses this problem explicitly. The ANSYS code does not have the capability for handling large strains and thus the resultant solution is inappropriate and therefore not able to be used as a comparative measure against PETROS. The PETROS code is amply verified by experiment and alternate analyses in the following references.

References (Reply 3.b.):

1. Atluri, S., Witmer, E. A. Leech, J. W., Morino, L., "PETROS III a Finite Difference Method and Program for the Calculation of Large Elastic-Plastic Dynamically-Induced Deformations of Multilayer Variable-Thickness Shells", BRL CR60 (MIT-ASRL TR 152-2), November 1971.

2. Morino, L., Leech, J. W., and Witmer, E. A., "PETROS 2: A New Finite-Difference Method and Program for the Calculation of Large Elastic Plastic Dynamically-Induced Deformations of General Thin Shells", BRL CR 12 (MIT-ASRL TR 152-1), December 1969. (In two parts: AD708773 and AD708774).

ADDITIONAL CLARIFICATION
TO WCAP-7832

1. Replace pages 3.1-14 and 3.1-15 with the attached superseding pages 3.1-14, 3.1-14a, 3.1-14b and 3.1-15.

2. ERRATA

   i) Figure 2.3-1: Change "Design Basis Earthquake" to "Safe Shutdown Earthquake".

   ii) Pg. 1.1-1: Last word should be "mixture".

   iii) Pg. 1.1-2: Fifth para., first sentence should read, "The 51 Series have 3388 U-Tubes of 0.875 in. O.D. and 0.050 in. nominal wall thickness; the D Series Steam Generator has 4674 U-Tubes of 0.75 in. O.D. and 0.043 in. nominal wall thickness."

   iv) Delete the character before "Figure 1.3-2" in that figure.

   v) Pg. 3.1-13: Delete "from Ref. [6]" from second line.

3. Substitute attached Table 3.1-2 for that in the WCAP.

Therefore the total allowable crack length is 0.64 inch for the 'D' series

3.1.6 TUBE THINNING

An investigation was performed to determine the margin of tube wall thinning which could be tolerated without exceeding ASME Code, Section III Faulted Condition stress limits when subjected to combined LOCA and SSE loads. Section 3.1.3 outlines the Faulted Condition limits; these are:

Allowable Primary Membrane Stress, P_m = 52,500 psi
Allowable combined Primary Membrane and Bending Stress, $P_m + P_B$ = 78,750 psi

A parametric study, varying the tube wall thickness showed that D Series tubes with a minimum wall thickness of:

t = 0.026 in. (0.75 in. nominal diameter tubing)

would have combined bending and membrane stresses of:

$P_m + P_B$ = 75,100 psi (0.75 in. nominal diameter)

which is less than the allowable limit.

For the 51 Series Steam Generator tubing (0.875 in nominal diameter and 0.050 in. nominal wall thickness) a simplified calculation to determine minimum uniform wall thickness based on combined LOCA and SSE loading conditions and ASME Code, Section III, Faulted Condition stress limits results in a value of 0.021 in. This thickness results in combined bending and membrane stress of:

$P_m + P_b$ = 72,800 psi (0.875 in. nominal diameter tube)

The analysis for the study (on the D Series tubing) was identical to that described earlier in Section 3.1.1, with the exception of the tube wall thickness being 26 mils. Figures 3.1-42 through 3.1-46 give the stresses at the various node locations, due to the LOCA rarefaction wave; Figures 3.1-47 through 3.1-51 give the stresses at the various node locations due to shaking caused by LOCA; Figure 3.1-52 shows the maximum stress intensity which occurs at Node 16.

The Primary Membrane Stress Intensity is a maximum at t = 0 seconds, when the tube is under the influence of its highest internal pressure. At this point in time:

$$P_m = 23{,}000 \text{ psi}$$

This stress is calculated from torus geometry equations, as applicable to the U-bend region using the smallest bend radius. The Primary Membrane plus Primary Bending Stress Intensity ($P_m + P_B$) is found to be a maximum at the location associated with node 16, shown in Figure 3.1-52 at t = .06 seconds after the primary coolant outlet line severance. This value, when combined with the maximum seismic bending stress of 5000 psi, is,

$$P_m + P_B = 75{,}100 \text{ psi}$$

Summary

The minimal wall thicknesses determined here are based on several degrees of conservatism. First, the maximum stress values which occur at different* locations in the tube bundle have been treated as if they acted at the same point. Second, the maximum stress levels resulting from each

* The various axial and circumferential (clock) positions, and the stress orientations at a specific point have been treated as an absolute summation

contributing load do not necessarily occur simultaneously; but are assumed to be simultaneous. Third, the ASME Faulted Condition stress limits are conservative when based on Engineering Stress-Strain Curves for determination of ultimate stress. A comparison of developed stresses for any given plastic strain in Figure 3.3-4 against that of Figure 3.3-5 illustrates this point.

The mimimum wall thicknesses given here were governed by the conservatively assumed stress state at a particular location in the tube bundle (Node 16, tangent to the curved, U-bend region). The minimum wall thickness required to sustain LOCA plus SSE loadings at other locations (e.g., straight section above the tube sheet: Node Location 1) would be substantially lower as can be seen in Figures 3.1-3 through 3.1-12 for various Nodal locations.

Summary

Table 3.1-2 summarizes tube wall thickness and the equivalent stresses generated by combined DBA plus SSE loads.

3.1.7 EXTERNAL PRESSURE EFFECTS

Subsequent to primary system blowdown, the differential pressure across the tubes will be secondary side pressure minus containment back pressure.

Westinghouse tests of the 51 series 7/8 in. diameter, 0.050 in. wall straight tube indicate that a collapse pressure of 6400 psi at room temperature was obtained, for annealed Inconel material of 51,000 psi yield strength, at 0% tube ovality. An analytical correlation based on plastic limit analysis was developed in order that extrapolation of test results to tubes of different yield strength and wall thickness would be possible. This correlation was applied to determine the predicted collapse pressure for straight Inconel tubing with minimum yield strength for the ASTM material at design temperature and minimum specified wall thickness. This results in a collapse pressure of approximately 3000 psi for 0% ovality and 1830 psi for the maximum allowable 5% ovality at 600°F. Tests on U-bend specimens

of different radii show that collapse pressure increases with reduced bend radius and is always higher than the straight tube due to toroidal surface curvature effects.

cc ~~TMA~~
JEMC

UNITED STATES
NUCLEAR REGULATORY COMMISSION
WASHINGTON, D. C. 20555

NOV 12 1975

Mr. C. Eicheldinger, Manager
Nuclear Safety Department
Westinghouse Electric Corporation
P. O. Box 355
Pittsburgh, Pennsylvania 15230

RECEIVED
NOV 17 1975
C. EICHELDINGER
PWR NUCLEAR SAFETY

Dear Mr. Eicheldinger:

To complete our review of Westinghouse Electric Corporation report WCAP-7832 (Non-proprietary) entitled, "Evaluation of Steam Generator Tube, Tube Sheet and Divider Plate Under Combined LOCA Plus SSE Conditions", additional information is required. The required information is identified in Enclosure 1.

To meet our review schedule, we need this additional information by December 19, 1975. If you cannot meet this schedule, please inform us within ten days after receipt of this letter of the date you plan to submit your response.

If you have any questions about our request for additional information, please contact us.

Sincerely,

D. B. Vassallo, Chief
Light Water Reactors
Project Branch 1-1
Division of Reactor Licensing

Enclosure:
Request for Additional
Information

NOV 12 1975

ENCLOSURE 1

MECHANICAL ENGINEERING BRANCH

OFFICE OF NUCLEAR REACTOR REGULATION

REQUEST FOR ADDITIONAL INFORMATION

WESTINGHOUSE REPORT: WCAP-7832

EVALUATION OF STEAM GENERATOR TUBE, TUBE SHEET AND DIVIDER PLATE UNDER COMBINED LOCA PLUS SSE CONDITIONS

1. Regarding your reply to Item 2.B.d of our request for additional information, dated August 12, 1974, explain the increase in strength of service exposed tubes with no intergranular corrosion as compared with tubes of origin material, as shown in Figure VII -5 (p. 24d) of your reply.

2. (a) Define the term "stress intensity."

   (b) Show that the maximum "membrane plus bending" stress intensities in healthy and thinned tubes are lower than the allowable stress limits when effects due to normal and upset operating conditions, such as flow induced vibration and vortex shedding, are included in the analysis.

3. (a) Indicate the allowable stress limit in membrane plus bending for the divider plate material.

   (b) Indicate the location in the divider plate where the maximum membrane plus bending stress intensity occurs, and show that it is below the limit in part (a).

Westinghouse Electric Corporation
Power Systems Company

PWR Systems Division
Box 355
Pittsburgh Pennsylvania 15230

December 19, 1975

NS-CE-885

Mr. D. B. Vassallo, Chief
Light Water Reactors
Project Branch 1-1
Division of Reactor Licensing
Attn: Mr. Raymond R. Maccary
Assistant Director for Engineering
Division of Systems Safety
Office of Nuclear Reactor Regulation
United States Nuclear Regulatory Commission
Washington, DC 20555

Dear Mr. Vassallo:

Enclosed are fifteen (15) copies of the additional information requested in your letter of November 12, 1975 in order to complete your review of Westinghouse Electric Corporation topical report WCAP-7832 (non-proprietary) entitled "Evaluation of Steam Generator Tube, Tubesheet and Divider Plate under Combined LOCA plus SSE Conditions."

WCAP-7832, submitted in December 1973, presents a detailed analysis of the steam generator structural design to demonstrate its capability to sustain stresses resulting from simultaneous LOCA and SSE loading conditions. We trust that your review of this added information will provide the desired clarification.

Your letter referred to your review schedule for this WCAP. Westinghouse wishes to be advised of the details of that schedule. This report has provided much of the material used mutually by the Technical Review Staff and by Westinghouse in the ongoing public hearings dealing with steam generator integrity and is expected to be instrumental to the eventual resolutions reached in those hearings.

Westinghouse considers that timely completion of your review and approval of this document would prove mutually beneficial for its use in safety analysis reports. We request that you consider this desire when setting the schedule for completion.

Very truly yours,

C. Eicheldinger

C. Eicheldinger, Manager
Nuclear Safety Department

CE/lz
Enclosures

ATTACHMENT

1. Your request for information regarding the apparent increase in strength of service exposed tubes compared to virgin material* is answered as follows. The lead plug tests which were referenced had as their objectives determination of possible significant changes in ductility as a function of surface exposure. All of the service exposed tubes without cracks came from one tube, and thus one heat of Inconel. The virgin material, on the other hand, was also from one different lot of Inconel. Thus the apparent differences in flow strength represent the normal variations in yield strength exhibited by Inconel 600 tubing. For example, a review of mill records for HAPD Inconel varied in yield strength from 38,500 to 65,500. This indicates that considerable variation in yield strength is typical of normal production material.

*Inconel tubing exposed to primary cooling chemistry for one year, W Forest Hills loop setup.

2a The term stress intensity is defined as per ASME Code paragraph NB-3213.11, Section III, 1974.

2b As per Section III of the ASME Code, the Faulted Condition must consider Primary Stresses. The Primary Stresses of LOCA + SSE are the result of the rarefaction wave, the LOCA shaking, and the SSE event. WCAP-7832 and related attachments addressed these stresses. Stresses due to tube vibration at 100% load were not considered in the WCAP due to their relative minor contribution. Investigation of these tube stresses for healthy Series 51 and Model D tubes shows that the maximum bending stresses are less than 3.6 ksi at the top of the U-Bend of the outermost tube. The bending stress due to tube vibration at the top tube support plate for each is 1 ksi. The top tube support is the location of maximum stress due to the LOCA + SSE event, and the addition of this tube vibration stress would produce a negligible effect. This is shown as follows: In a thinned tube this bending due to vibration will result in a stress of 1.6 ksi for a model D tube thinned to .026 "and a stress of 2.2 ksi for a Series 51 tube thinned to .021".

The worst of all the above cases, the thinned Series 51 tube, will result in a total Stress Intensity of 77.3 ksi, this is less than the Section III Code allowable of 78.7 ksi.

3a The allowable stress limit in membrane plus bending for the divider plate material for Faulted Conditions is taken from Appendix F of Section III of the ASME Code and is 1.5(.7)(Su) = 72.4 KSI.

3b By virtue of the full constraint at the periphery of the divider plate, the bending stresses in the divider plate are secondary in nature. This categorization of stress is appropriate as it has been shown that the perimeter of the divider plate meets Section III code allowable for primary membrane stress.